

DEPARTMENT OF COMMERCE
FREDERICK H. MUELLER, Secretary

WEATHER BUREAU
F. W. REICHELDERFER, Chief

MONTHLY WEATHER REVIEW

JAMES E. CASKEY, JR., Editor

Volume 87
Number 6

JUNE 1959

Closed August 15, 1959
Issued September 15, 1959

A SEQUENCE OF TORNADO DAMAGE PATTERNS

Ferguson Hall and Robert D. Brewer

U.S. Weather Bureau, Washington, D.C.

[Manuscript received April 6, 1959; revised June 8, 1959]

ABSTRACT

An investigation is made of the patterns of damage associated with a series of tornadoes in west-central Wisconsin on June 4, 1958. Three flow models are presented to account for the different patterns exhibited in different portions of the paths.

1. INTRODUCTION

The system of tornadoes which struck west-central Wisconsin on the afternoon of June 4, 1958, passed over extensive forest areas, and left a sequence of damage patterns perhaps unique in recent years.¹ The storm system as a whole produced at least five major damage paths running in an east-northeasterly direction. The first and longest, and the one which accounted for severe damage to the village of Colfax, was 35 miles long, and although characteristically narrow over most of its extent, eventually widened into a 1½-mile path of almost total destruction. Each successive tornado of the system began to the south of the previous one, and at about the time the latter was reaching the end of its course. The second of the series produced a somewhat shorter path of about 17 miles, but was equally violent and caused severe damage to the northern outskirts of the city of Chippewa Falls. The paths are shown in figure 1.

2. DAMAGE PATTERNS

The damage patterns were recorded by a series of aerial photographs obtained with the assistance of Prof. Gilbert

Tanner of the Wisconsin State College at Eau Claire. Some 130 photographs were taken along the paths of the first and second tornadoes of the system. Over large segments of the paths the forest cover was adequate to permit quite accurate reconstruction of the damage patterns, even though, in the intervening open fields, no sign of damage was recognizable from the air.

The first tornado of the series was sighted as it touched down at about 6 p.m. south of the village of Woodville. From visual reports it seems evident that at this stage the storm consisted of a distinct and typical tornado funnel. Almost immediately after reaching the ground it struck the wooded area shown in figure 2. Although the tornado's path was almost exactly centered over this wooded section, it can be seen from the photograph that damage was much more complete in the southern half (lower part of picture), where the storm's translational speed of about 50 m.p.h. was added to the rotational motion (and of course was subtracted in the northern half).² A reconstruction of this damage pattern and those immediately following is shown in figure 3, where arrows represent fallen tree directions. In many instances the trees lay crossed over one another, as indicated in the sketch, and

¹ Somewhat similar patterns were recorded in Europe by J. Letzmann [1].

² See a discussion of this effect by G. W. Reynolds [2].

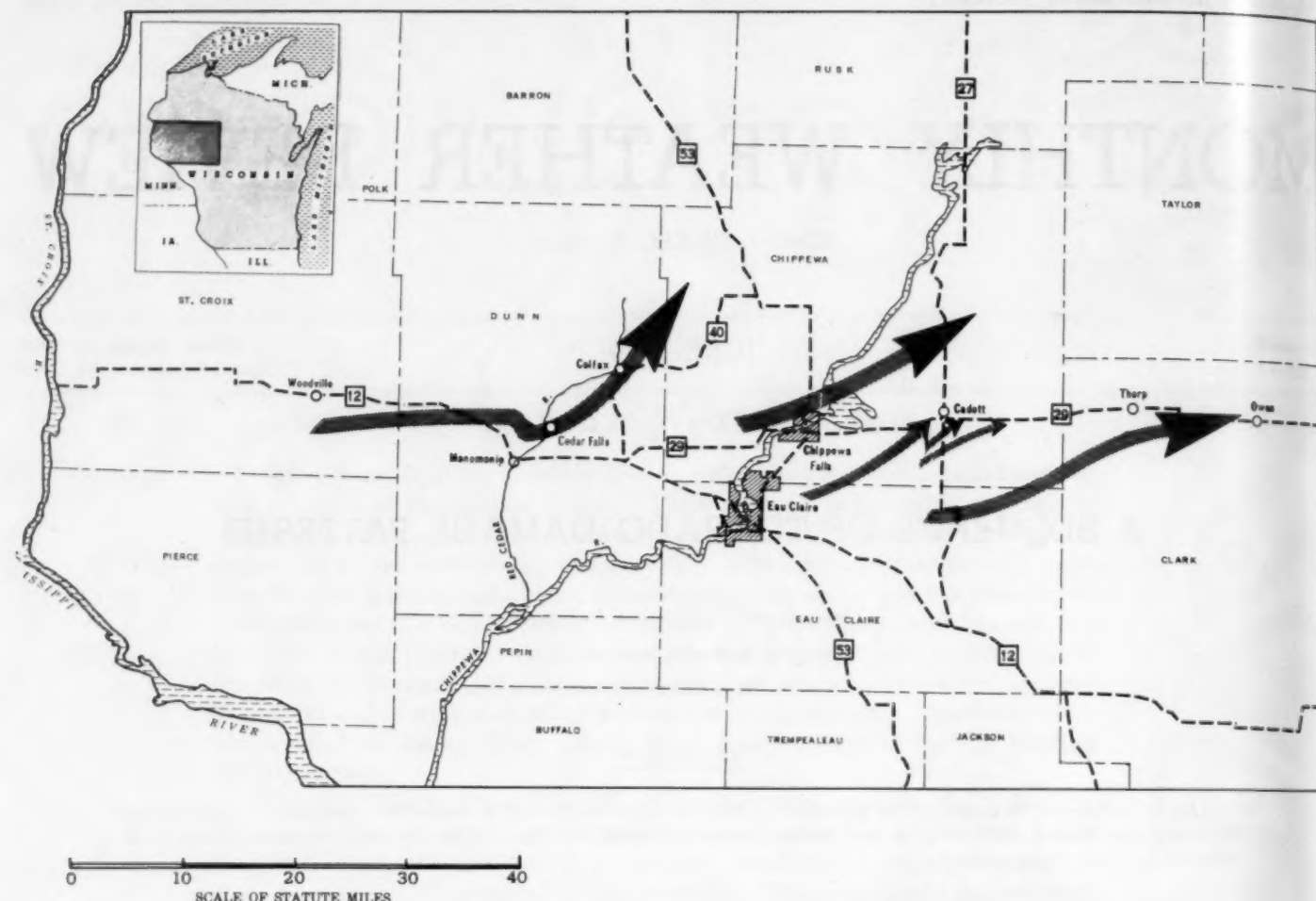


FIGURE 1.—Paths of major tornadoes of storm system.

in all such cases the sequence of directions in which the trees fell corresponded to what one would expect from the passage of a compact cyclonically rotating vortex. As can also be seen, the "reverse" flow along the northern side of the path became much less prominent as the storm progressed, suggesting that rotation had slowed somewhat so that the translational speed was more effective in countering the backward-moving component, or that the translation was much faster. This feature was an early indication of the highly variable character of the storm patterns which was typical of the entire track.

Pronounced damage patterns were infrequent for the next 8 miles of the path, and the storm may have been on the ground only intermittently or may have missed most of the heavily wooded areas. However, at about mile 7 another wooded tract was struck, apparently head-on, and again the pattern, as can be seen in figure 4, leaves unmistakable evidence of a well-formed and classical tornado funnel.

Between miles 11 and 16 the character of the pattern seemed to change. There was almost none of the marks of a rotating core that had been obvious earlier. Rather, the predominant feature was what might be called a

"herringbone" pattern, with the fallen trees directed forward and inward toward a sharp line of separation (at this line the trees sometimes even crossed each other on falling). The reconstructed damage patterns along this portion of the path are given in figure 5. Such patterns suggest the passage of a fast-moving center of strong inflow or convergence, with only a faint suggestion, on the northern side of the path, of the "reverse" flow associated with a funnel.

Continuing along the path, the pattern of the next few miles (roughly miles 17 to 19, fig. 6) returned to the general appearance of that seen in the later part of figure 3, where a strong forward flow along the southern edge of the path accompanied a rather weak and confused reverse flow along the northern edge of damage, all suggestive of modest rotational speeds coupled with pronounced forward movement. But beginning at mile 19 and continuing through mile 21 the full rotary pattern again became well marked, presumably due to an increase in vortex speed or to a slowing down in forward motion, or to both. The reconstructed damage pattern for this segment is given in figure 6. Not only did the pronounced rotation reappear, but the path showed an abrupt change



FIGURE 2.—Damage pattern in forested area where tornado first touched down.

in direction. As one explanation, the funnel may have continued toward the northeast, but then turned sharply southward and thence back on an eastward course. Alternatively, the original funnel may have dissolved as it moved northeastward, to be replaced by another forming to the south, as was the case on a much larger scale with the individual storms of the system, as mentioned earlier. Figure 7 is a photograph of the destruction which oc-

curred at point "A" of figure 6, and illustrates the circularity of the pattern. Also significant here is the sharp demarcation between destroyed and undamaged forest.

After thus deviating in its course, the storm crossed the Red Cedar River and struck the village of Cedar Falls, then continued its march to the east-northeast toward Colfax, some 8 miles distant. The area here is intensively farmed and the infrequent wooded sites in the storm's

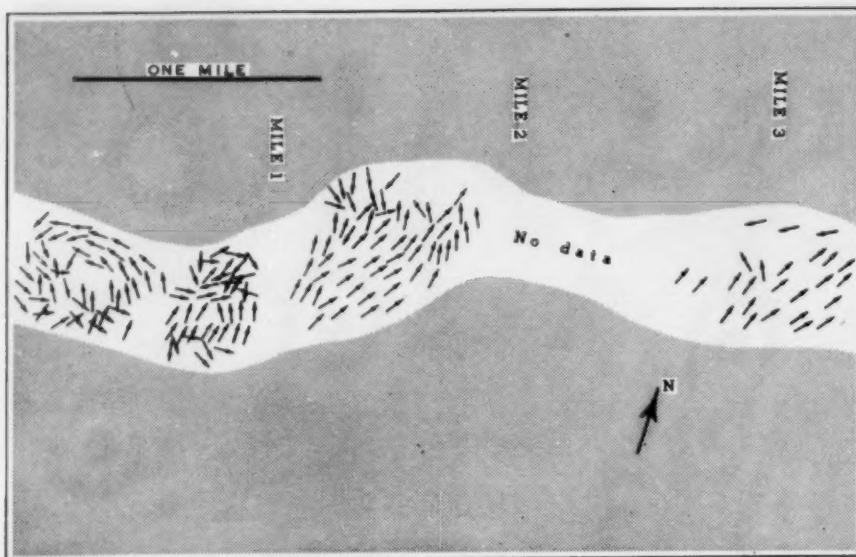


FIGURE 3. (At left)—Reconstructed damage pattern over first segment of tornado path. Arrows represent fallen trees.

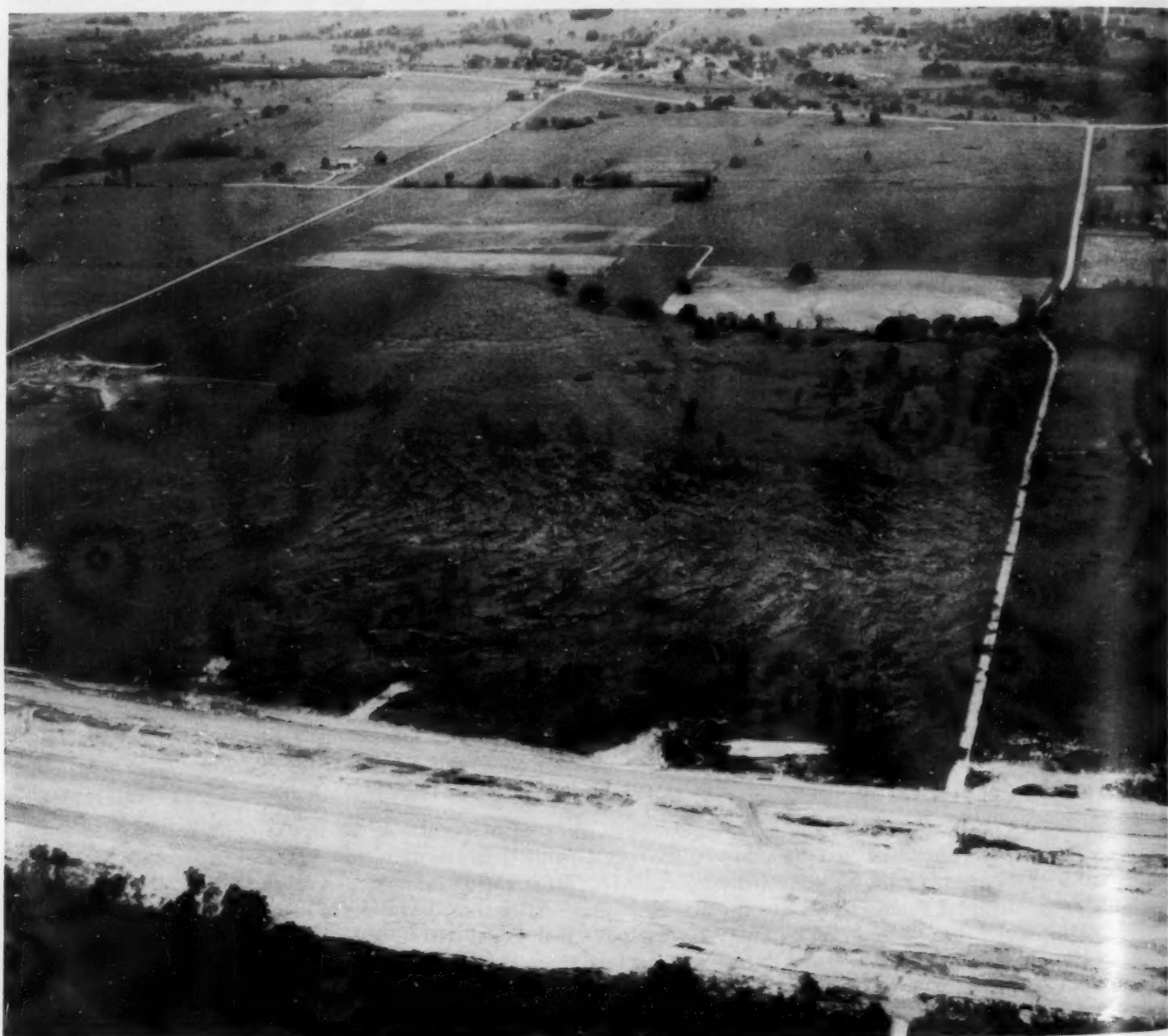


FIGURE 4. (Below)—Damage pattern showing distinct circularity.

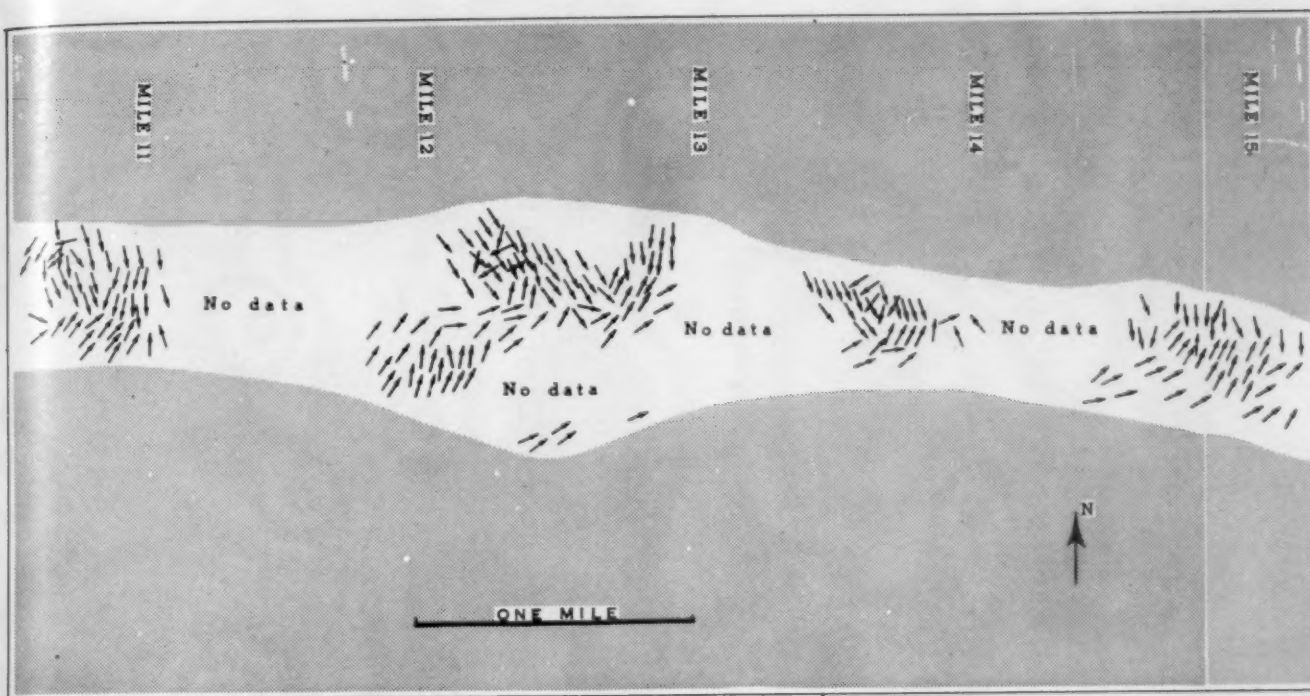


FIGURE 5.—Reconstructed damage pattern of the "herringbone" type.

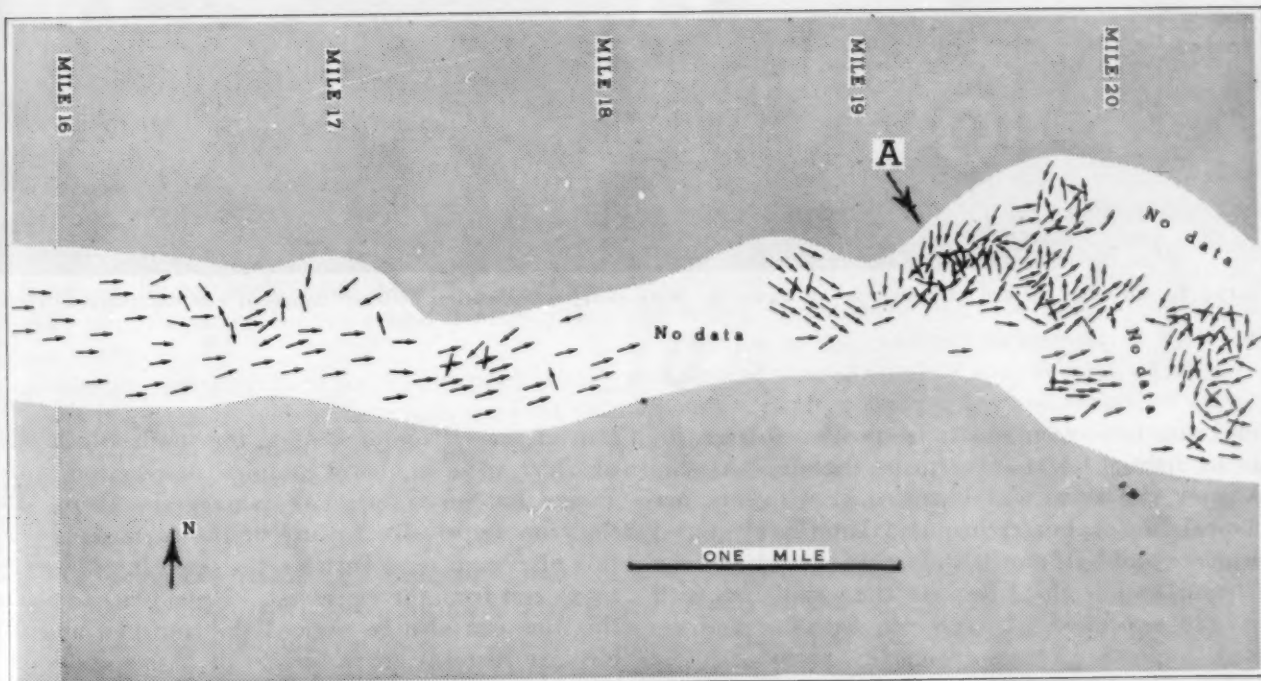


FIGURE 6.—Reconstructed pattern near midpoint of path.



FIGURE 7.—Circular pattern at point "A" of figure 6. Note sharp demarcation between damaged and undamaged trees.

path were, with two exceptions to be mentioned later, inadequate to define a clear-cut damage pattern. At this time, however, the storm was described by witnesses, not as a classical funnel, but rather as a huge bowl-shaped protuberance about half a mile wide, that extended to the ground from the low cloud deck of the squall line with which it was associated. Heavy rain preceded and accompanied the storm passage during this period.

The last 6 miles of the storm's path (miles 29 to 35) are pictured in figure 8. The shaded area is the built-up sec-

tion of the village of Colfax, the southeastern one-third of which suffered almost complete destruction, with widespread but more irregular damage elsewhere. Perhaps the most impressive feature of the patterns is the sharp line of demarcation between the opposing flows from the north and from the southwest. From place to place along this line can also be noticed the confused and at times circular patterns characteristic of high-speed vortex motion. Substantial alterations in pattern as the storm progressed are quite noticeable and might indicate highly

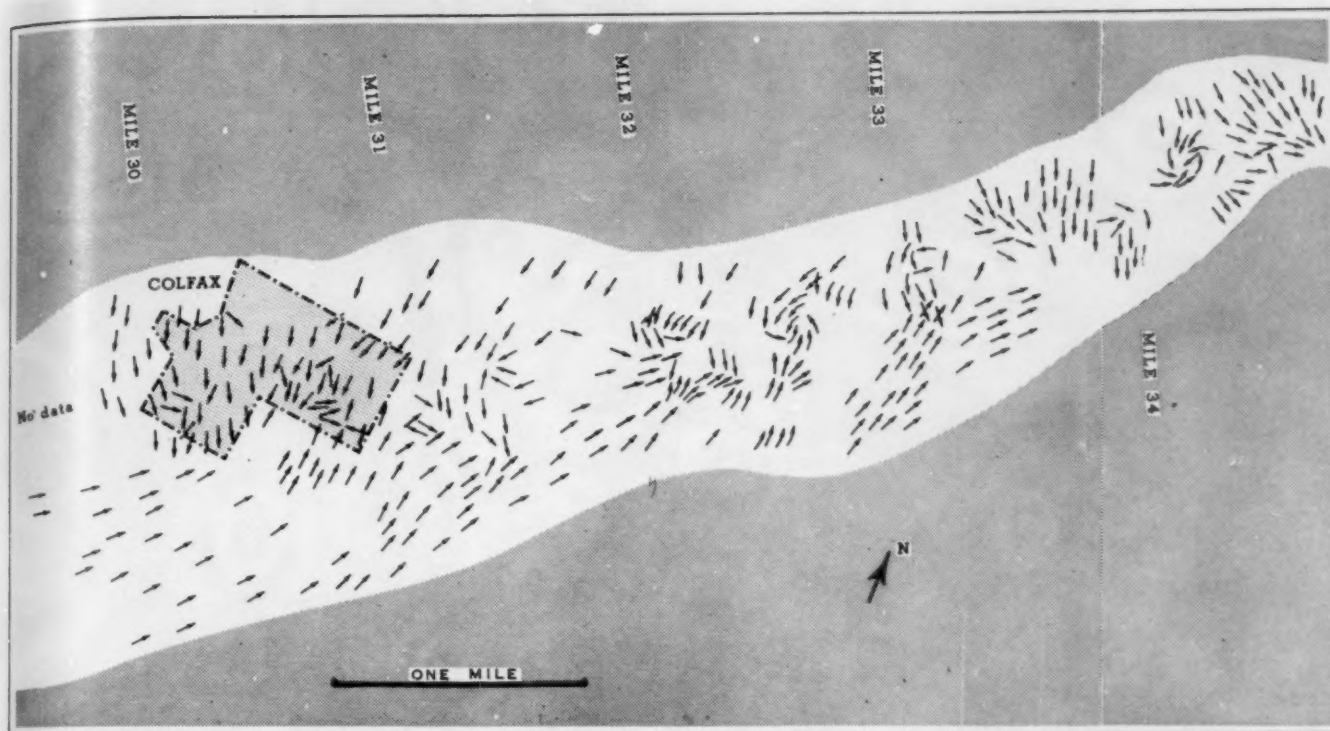


FIGURE 8.—Reconstructed pattern of final portion of path. Built-up portion of village of Colfax shaded.

unsteady storm structure, except that here the terrain is quite rolling or even hilly, and may have been sufficient to distort the flow. Taken as a whole, however, the patterns suggest a central high-speed funnel or vortex surrounded by an intense cyclonic circulation giving destructive winds out to a radius of $\frac{3}{4}$ mile. The highly convergent appearance of the damage also suggests, however, the presence of intense inflow toward the center of the storm sufficient to distort the pattern normally produced by a moving rotary system of winds. Figure 9 shows a view of Colfax, looking northward from the southern village limits.

3. FLOW MODELS

Three idealized flow models were constructed to see how well they might account for the actual damage patterns. These consisted of—

(a) a translation speed of 25 m.p.s. (56 m.p.h.) combined with a VR vortex in which the winds were set at 55 m.p.s. (123 m.p.h.) at a radius of 100 m. from the center and decreased in proportion to increasing radius;

(b) translation combined with a sink with converging wind of 60 m.p.s. (134 m.p.h.) at the 100 m. radius and decreasing with increasing radius in the same fashion;

(c) translation combined with both vortex and sink (this of double the above strength).

The sequences of winds which would be experienced at the surface during the passage of these systems are shown

in figure 10. Model (a) would undoubtedly account for the patterns of both figure 3 and figure 6, where rotation and translation seem predominant and the degree of "circularity" of the pattern would depend upon the forward speed of the system relative to the intensity of the vortex circulation. Thus the strongly circular patterns at the beginning of figure 3, where the tornado first touched ground, and at point "A" of figure 6 imply high vortex speeds or low forward motion. In the first case it seems possible that the funnel may have built up to very high speed just before touching the ground. Then due to surface friction this speed may have been reduced to give the translational type of pattern immediately following and continuing for the next mile or two. In the case of the circular patterns of figure 6, a marked deceleration of the system would seem likely, accompanying the change in direction or alternatively in connection with the substitution of a second funnel for the first. This furnishes a possible explanation for the recurrence of circularity, but does not necessarily account for the sharp demarcation between damaged and undamaged forest noted in figure 7. The latter suggests the funnel was more in the nature of a spinning column of air, perhaps in solid rotation, moving through a relatively undisturbed environment not partaking of the tornado circulation. It is possible that this particular vortex was indeed dying out, as suggested previously, and was merely "coasting," separated from the VR circulation which was then attached



FIGURE 9.—View from south of part of damage at Colfax, Wis.

to the newly developing funnel. Behavior similar to this has been observed in the past where little wind has been felt immediately outside the funnel itself.

Model (b), representing strong inflow toward a moving center (implying a major sustained updraft into the storm center), seems consistent with the herringbone damage patterns of figure 5, where the survey found no significant evidence of rotation. If this interpretation is correct, the funnel must have been lifted off the ground accompanying a resurgence in cloud formation taking place at or near the storm center. An unbalance between pressure gradient and winds, perhaps caused by friction, may have resulted in strong upward motion around the funnel, pulling it upward—possibly the same mechanism responsible for the formation of the "collar" or "ruffle"

near the cloud base noticed in several other tornadoes.

The final stage of the storm's course, as illustrated in figure 8, seems to differ substantially from the earlier patterns, and is most closely approximated by the three-way combination of rotation, translation, and inflow of model (c). This model appears to explain the flow from the southwest along the bottom of the path separated quite sharply from the flow from the north along the upper portion. A number of observers in this portion of the storm path reported marked wind shifts as the storm approached closely. At first, winds were from an easterly direction, with enough force to blow over smaller trees. A few seconds later the main storm struck with winds from a southwesterly direction, and with much greater force. Such a sequence would not be compatible with

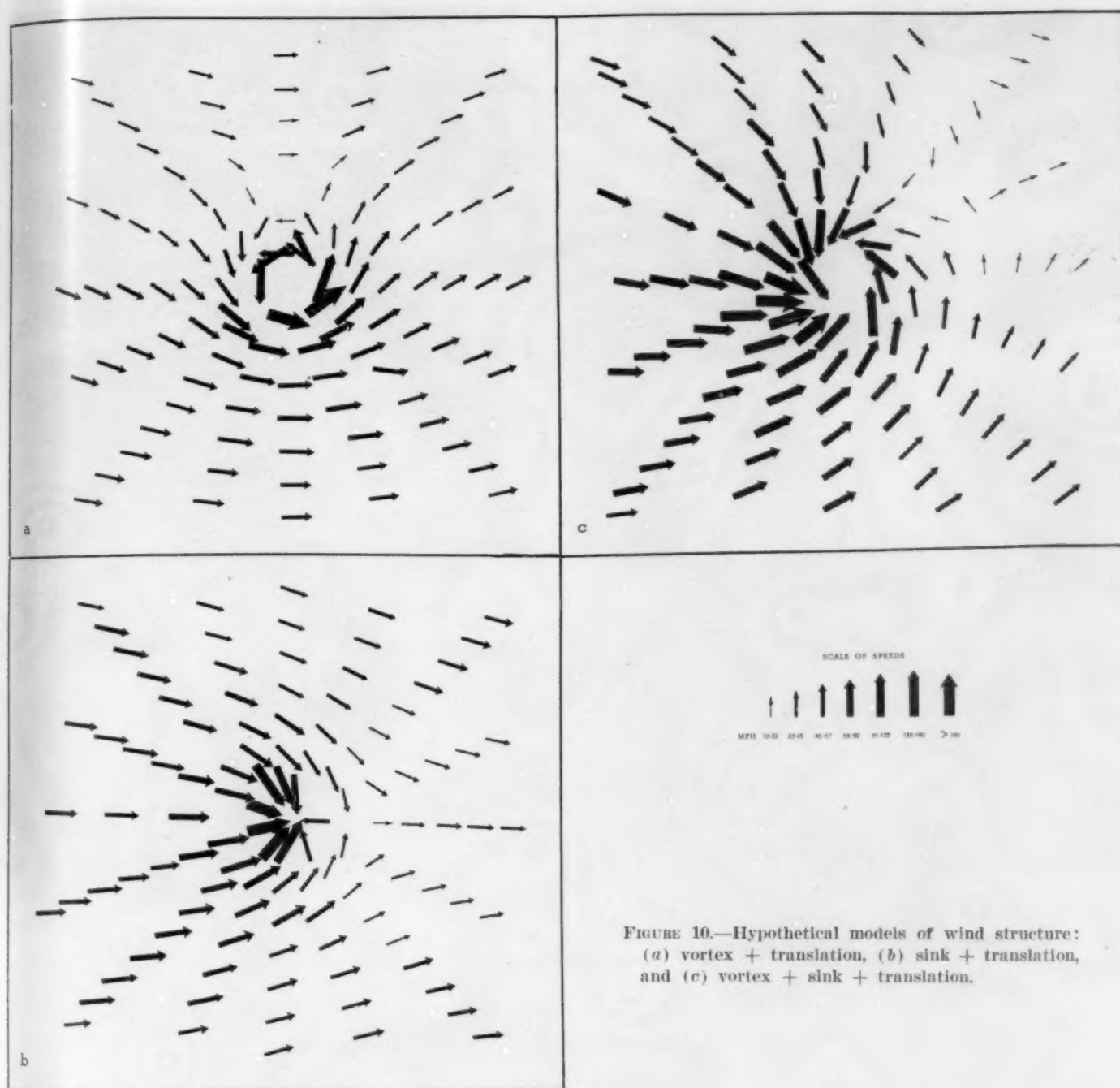


FIGURE 10.—Hypothetical models of wind structure: (a) vortex + translation, (b) sink + translation, and (c) vortex + sink + translation.

model (a), but might very well occur with models (b) and (c) near the axis of motion, provided the final inflow speeds greatly exceeded the translational and rotational speeds. Thus, due to the high rate of inflow, the wind would blow back toward the approaching center for a brief period before the center passed, to be followed, south of the center, by strong flow in the direction of general storm movement.

The unsteady state of the storm during this final stage is evident from the variability of damage patterns shown

in figure 8. For this reason no one hypothetical model can be expected to provide an exact "fit" to the observed patterns. Also, as has been mentioned, the rolling and hilly topography in this section may have had a decided influence on resulting damage by producing distortion of the wind flow.

A flow pattern of quite different character is illustrated in figure 11, which shows a distinct fan-shaped or "crow's-foot" distribution of felled trees. This pattern occurred at mile 26, and a similar one occurred a mile earlier. Over

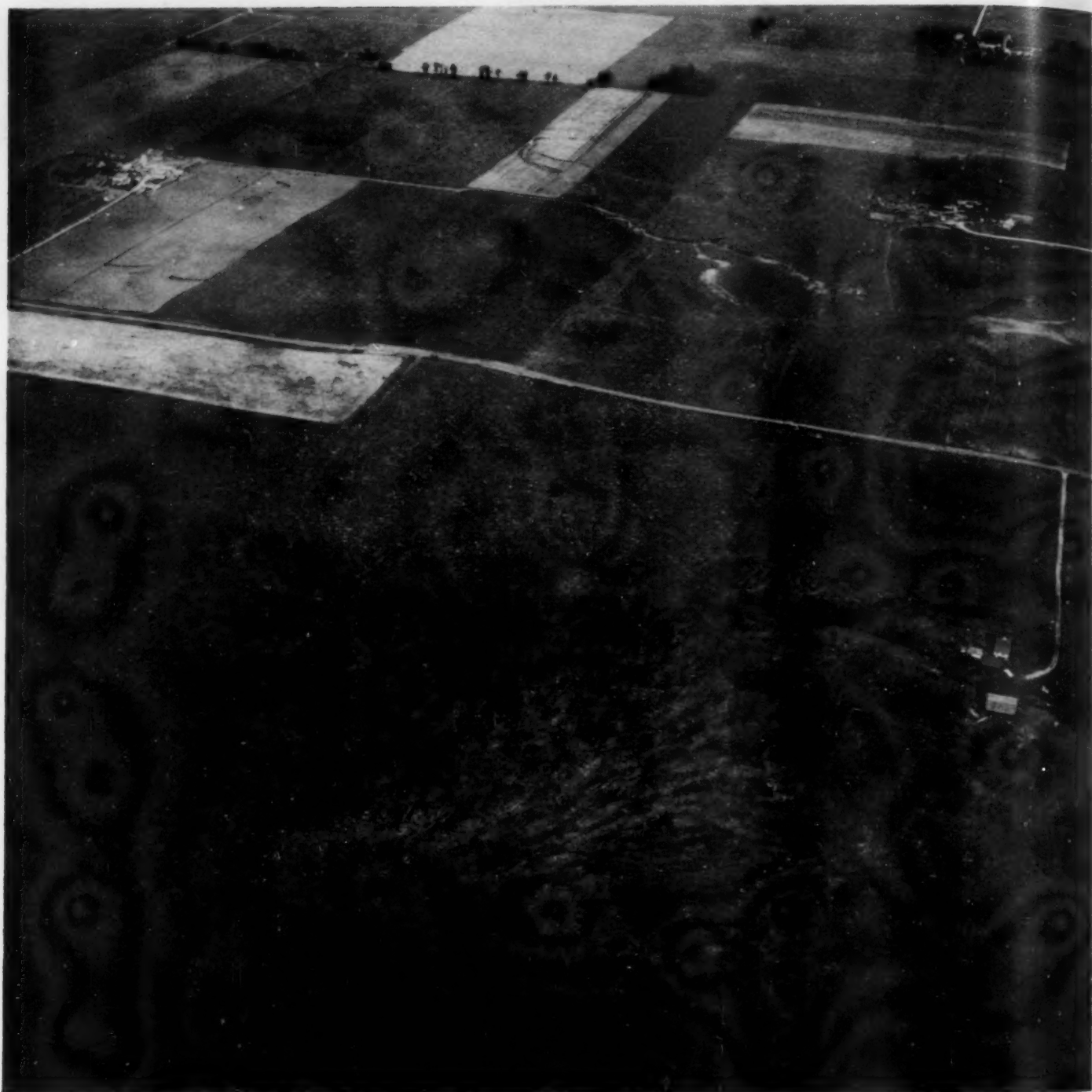


FIGURE 11.—Fan-shaped damage pattern.

level terrain one would undoubtedly conclude that such a pattern was produced by a combination of a source (downdraft) and translation. In both of these cases, however, the pattern occurred on hills (wooded portion in fig. 11), leaving the possibility that it was due to the terrain.

REFERENCES

1. J. Letzmann, "Fortschreitende Luftwirbel," *Meteorologische Zeitschrift*, vol. 42, Jan. 1925, pp. 42-52.
2. G. W. Reynolds, "A Common Wind Damage Pattern in Relation to the Classical Tornado," *Bulletin of the American Meteorological Society*, vol. 38, No. 1, Jan. 1957, pp. 1-5.

MEAN SOUNDINGS FOR THE GULF OF MEXICO AREA

Paul J. Hebert and C. L. Jordan

Department of Meteorology, Florida State University¹

[Manuscript received March 9, 1959]

ABSTRACT

Mean aerological data for the Gulf of Mexico area have been prepared from 10-year records for three stations. Mean monthly height, temperature, and relative humidity data are tabulated for constant pressure surfaces. More detailed information, including density, potential temperature, and specific humidity, is shown for the mean "hurricane season" sounding. The mean data are compared with those previously presented for the West Indies area and some of the interesting climatological features are discussed.

1. INTRODUCTION

Recently, mean sounding data have been presented for the West Indies area based on 10-year records for Miami, Fla., San Juan, P.R., and Swan Island [1]. At about the same time, mean aerological data were being prepared for individual U.S. Weather Bureau and cooperative stations for the same 10-year period, 1946-55 [2]. Since the availability of these mean data for the individual stations greatly simplifies the preparation of mean soundings for geographical areas, it was decided to prepare, for comparative purposes, mean soundings for the Gulf of Mexico area by combining the published means for Brownsville, Tex., Burrwood-New Orleans,² La., and Havana, Cuba. This new set of data for a slightly different geographical area (fig. 1) should be useful as a check on the representativeness of the mean West Indies data [1], and also provide information on seasonal variations of temperature, pressure, and humidity over the northern Gulf of Mexico.

2. PROCESSING OF DATA

In preparing the mean sounding data for the Gulf of Mexico area, the information was processed in a somewhat different manner than that employed in computing the mean West Indies sounding. Detailed information on the length of record and the techniques employed in reducing bias in the monthly means at the upper levels at the individual stations is given in [2]. In contrast to the mean West Indies soundings, the pressure-height data for the Gulf soundings were not computed from the mean temperature and humidity data; the height data for the standard pressure surfaces were obtained by simply averaging the reported heights at the individual levels. Checks made in [1] suggest that only very minor inconsistencies are introduced by treating the data in this way.

¹This report was prepared with the support of the U.S. Weather Bureau and was preprinted as National Hurricane Research Project Report No. 30, April 1959.

²Data taken at New Orleans for the period Jan. 1947-July 1950 and at Burrwood for Jan.-Dec. 1946 and Aug. 1950-Dec. 1955 were combined in preparing the mean data [2]. This combined record will be referred to as Burrwood in the subsequent discussion.

To the extent possible, mean data are shown for all standard levels up to 30 mb, as in [1], although relatively few observations reached this level in the earlier years. The mean surface pressures were reduced to mean sea level pressures simply by considering the mean elevation of the three stations and the mean temperature in the layer near the surface.

The mean values are based entirely on the 0300 GMT observations in both sets of data so that radiation errors, noted in radiosonde records in the past [3], need not be considered. The observations were scheduled at local times varying from approximately 10:30 p.m. at San Juan to about 8:30 p.m. at Brownsville. Since relatively small mean diurnal differences can be expected over a 2-hour period [3] and since any effect of this type introduced by the San Juan and Brownsville data would tend to be reduced by the data from the other stations, which are all within 10° longitude of each other, it is felt that diurnal differences can safely be neglected in comparing the Gulf and West Indies soundings.

3. THE MEAN AEROLOGICAL DATA

The monthly and annual temperature, height, and relative humidity data for the standard pressure surfaces for the Gulf of Mexico area, obtained by averaging the

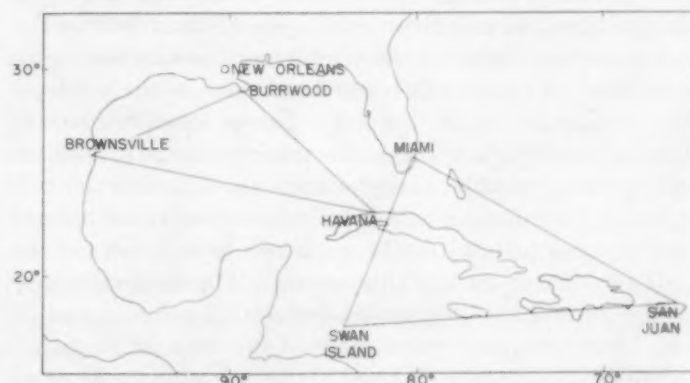


FIGURE 1.—Location map for stations used in the preparation of mean soundings for the Gulf of Mexico and West Indies areas.

TABLE 1.—*Mean temperature (° C.) at standard pressure surfaces for Gulf of Mexico area. All values above the dashed line are negative*

Pressure (mb.)	January	February	March	April	May	June	July	August	September	October	November	December	Annual
30	56.0	57.3	56.5	53.1	53.1	51.5	52.7	52.5	54.0	54.3	55.6	54.3	54.3
40	60.6	60.7	60.3	57.2	55.7	55.7	56.2	56.5	57.3	58.5	59.6	58.1	58.1
50	65.5	64.4	65.2	62.1	59.3	59.1	58.8	59.0	59.3	60.4	61.9	63.5	61.5
60	69.5	68.9	69.7	66.5	63.4	62.6	61.9	61.9	62.5	63.4	65.5	67.1	65.2
70	74.0	73.0	73.3	73.0	70.2	69.1	67.1	67.5	68.3	69.0	71.7	72.2	70.8
80	72.9	71.8	72.0	69.9	71.1	72.7	70.2	71.0	73.1	73.8	72.8	71.7	71.9
90	68.0	67.3	67.3	66.4	68.4	71.1	70.3	70.5	72.0	71.2	71.1	69.7	69.4
100	63.4	62.7	63.3	63.5	65.3	66.5	66.7	66.2	66.6	66.3	66.2	64.9	65.1
125	59.9	58.9	59.7	60.7	60.9	60.9	61.2	60.4	60.4	60.4	61.4	61.4	60.5
150	56.3	55.8	56.3	56.9	56.0	54.9	55.1	54.2	53.9	54.7	56.1	57.0	55.6
175	47.6	48.2	47.8	47.3	45.6	43.4	43.2	42.6	43.9	45.7	47.2	45.4	45.4
200	38.5	39.2	38.4	37.8	36.1	33.6	33.2	32.6	32.7	34.4	36.4	37.8	35.9
250	30.3	30.9	29.9	29.5	27.8	25.2	24.8	24.3	24.1	26.3	28.2	29.6	27.6
300	23.0	23.6	22.5	22.3	20.6	18.1	17.7	17.3	17.2	19.2	21.0	22.3	20.4
350	16.5	17.3	16.1	15.9	14.3	12.0	11.8	11.4	11.3	13.0	14.8	16.0	14.2
400	10.8	11.7	10.4	10.3	8.8	6.9	6.8	6.4	6.3	7.7	9.4	10.5	8.8
450	5.9	6.8	5.4	5.3	4.0	2.3	2.4	2.0	1.9	3.1	4.6	5.7	4.1
500	1.6	2.5	1.0	.8	.4	1.7	1.5	2.1	2.0	.9	1.4	.1	.1
600	2.2	1.5	3.2	3.4	4.6	5.6	5.4	5.8	5.7	4.6	3.3	2.4	4.0
650	5.6	5.1	6.8	7.0	8.3	9.1	9.0	9.4	9.1	8.0	6.7	5.6	7.5
700	8.3	7.9	9.7	10.1	11.6	12.4	12.4	12.7	12.2	10.9	9.4	8.4	10.5
750	10.4	10.0	11.8	12.7	14.4	15.4	15.6	15.8	15.1	13.3	11.6	10.6	13.1
800	11.9	11.6	13.8	15.0	17.1	18.3	18.6	18.5	17.9	15.7	13.4	12.2	15.3
850	13.6	13.5	15.5	17.2	19.7	20.9	21.4	21.7	20.7	18.3	15.3	14.0	17.8
900	15.3	15.5	17.3	19.2	20.6	23.3	23.8	24.2	23.4	21.0	17.6	16.0	18.8
950	17.1	17.5	19.3	21.4	24.0	25.8	26.2	26.6	25.8	23.5	19.9	17.9	22.1
1,000	16.7	17.2	19.1	21.6	24.1	26.0	26.5	26.8	25.8	23.1	19.4	17.3	22.0
Sfc.													

TABLE 2.—*Mean heights of standard pressure surfaces (meters) for Gulf of Mexico area. Sea level pressure (SLP) is given in millibars*

Pressure (mb.)	January	February	March	April	May	June	July	August	September	October	November	December	Annual
30	23,753	23,738	23,739	23,603	23,603	24,106	24,085	24,071	23,927	23,814	23,773	23,891	
40	21,936	21,905	21,928	22,000	22,074	22,179	22,250	22,264	22,219	22,106	21,983	21,957	
50	20,527	20,515	20,554	20,610	20,668	20,771	20,843	20,860	20,818	20,706	20,592	20,553	20,668
60	19,427	19,419	19,453	19,497	19,555	19,642	19,707	19,723	19,678	19,577	19,477	19,440	19,550
80	17,744	17,730	17,760	17,787	17,829	17,903	17,954	17,966	17,929	17,839	17,761	17,728	17,828
100	16,448	16,426	16,450	16,471	16,509	16,583	16,618	16,636	16,609	16,538	16,457	16,441	16,516
125	15,116	15,096	15,127	15,136	15,187	15,272	15,295	15,314	15,305	15,225	15,145	15,115	15,194
150	14,005	13,982	14,017	14,023	14,081	14,186	14,204	14,220	14,211	14,140	14,055	14,007	14,094
175	13,050	13,020	13,058	13,072	13,137	13,270	13,256	13,273	13,264	13,193	13,111	13,061	13,147
200	12,211	12,177	12,214	12,236	12,297	12,395	12,417	12,430	12,422	12,351	12,272	12,224	12,304
250	10,768	10,734	10,770	10,792	10,845	10,932	10,953	10,962	10,950	10,887	10,821	10,779	10,849
300	9,540	9,511	9,542	9,560	9,605	9,679	9,698	9,704	9,690	9,638	9,582	9,608	
350	8,463	8,436	8,463	8,479	8,517	8,578	8,595	8,600	8,585	8,543	8,496	8,468	8,519
400	7,500	7,475	7,498	7,512	7,544	7,595	7,603	7,614	7,598	7,563	7,524	7,502	7,544
450	6,631	6,609	6,628	6,642	6,668	6,711	6,727	6,728	6,713	6,684	6,650	6,632	6,669
500	5,822	5,803	5,818	5,831	5,852	5,888	5,903	5,903	5,886	5,863	5,835	5,821	5,852
550	5,084	5,068	5,078	5,090	5,108	5,140	5,155	5,155	5,137	5,116	5,093	5,082	5,109
600	4,396	4,381	4,389	4,400	4,414	4,441	4,456	4,453	4,437	4,420	4,401	4,393	4,415
650	3,757	3,745	3,748	3,759	3,771	3,795	3,809	3,806	3,791	3,777	3,761	3,755	3,773
700	3,151	3,141	3,140	3,150	3,159	3,180	3,196	3,191	3,175	3,163	3,151	3,148	3,162
750	2,589	2,581	2,576	2,585	2,591	2,609	2,623	2,617	2,604	2,597	2,587	2,597	2,600
800	2,048	2,040	2,032	2,040	2,042	2,060	2,075	2,069	2,055	2,049	2,043	2,045	2,050
850	1,541	1,534	1,523	1,529	1,527	1,543	1,556	1,550	1,537	1,536	1,538	1,537	1,537
900	1,061	1,055	1,059	1,042	1,036	1,049	1,063	1,055	1,044	1,048	1,051	1,057	1,050
950	608	601	583	582	573	584	594	587	579	585	594	603	598
1,000	167	159	138	134	119	127	138	130	122	134	146	160	140
SLP	1,020	1,019	1,016	1,015	1,014	1,014	1,015	1,015	1,014	1,015	1,017	1,019	1,016

data for the three stations (fig. 1), are shown in tables 1-3. Seasonal changes at the individual stations, especially Burrwood and Brownsville, are quite large and the mean monthly data for the winter months can hardly be considered as representative of conditions in the whole of the triangle shown in figure 1. In the summer months, thermal conditions at the three stations are very similar and month-to-month changes are small. The mean soundings are, therefore, much more representative of normal conditions which would be expected over much of the Gulf of Mexico during this season. The major portion of the subsequent discussion deals with summer conditions; however, some use is made of the data for the other months in comparing seasonal variations over the Gulf of Mexico with those indicated for the West Indies area in [1].

TABLE 3.—*Mean humidity (percent) at standard pressure surfaces for Gulf of Mexico area*

Pressure (mb.)	January	February	March	April	May	June	July	August	September	October	November	December	Annual
400	30	33	32	33	34	35	42	41	40	33	31	32	35
450	28	31	30	32	32	36	43	42	41	32	29	30	34
500	26	30	30	32	34	38	46	43	43	33	29	30	36
550	26	30	30	32	35	40	49	47	46	34	30	29	38
600	27	32	31	33	37	42	51	49	50	38	32	31	38
650	30	33	31	34	38	43	53	51	52	40	34	32	39
700	33	35	32	36	40	46	54	53	55	43	37	36	42
750	38	38	37	41	45	49	56	56	59	47	42	41	46
800	48	47	44	47	52	56	59	60	63	55	49	49	52
850	58	57	53	54	58	61	64	63	68	62	57	57	59
900	67	66	63	62	64	67	68	68	71	68	66	66	66
950	74	73	71	73	73	75	76	76	73	72	74	74	79
1,000	78	70	69	79	81	81	81	80	81	77	75	77	79
Sfc.	84	82	83	82	84	84	83	83	84	83	82	83	83

TABLE 4.—Mean Gulf of Mexico "hurricane season" sounding data for isobaric surfaces. Mean values of height (H), temperature (T), density (ρ), potential temperature (θ), equivalent potential temperature (θ_E), relative humidity (f), and specific humidity (q) are tabulated. Deviations (Δ) of mean Gulf of Mexico sounding data from mean West Indies sounding data are given for all of the above quantities

P (mb.)	H (ft.)	H (m.)	ΔH (m.)	T (° C.)	ΔT (° C.)	ρ (kg./m. ³)	$\Delta \rho$ (kg./m. ³)	θ (° A.)	$\Delta \theta$ (° A.)	θ_E (° A.)	$\Delta \theta_E$ (° A.)	f (%)	Δf (%)	q (g./kg.)	Δq (g./kg.)
10	79,005	24,087	116	-52.2	1.8	0.047	-0.001	604	7						
10	72,965	22,246	107	-56.1	1.2	.064	-.001	531	7						
10	68,355	20,840	97	-59.0	1.6	.080	-.002	507	7						
10	64,625	19,703	83	-62.1	1.8	.099	-.001	474	6						
10	58,875	17,950	63	-67.6	2.2	.136	-.001	425	7						
10	54,515	16,621	53	-71.4	2.1	.173	-.001	391	5						
10	50,200	15,305	45	-70.9	1.3	.215	-.002	368	4						
10	46,610	14,211	34	-66.5	1.1	.233	-.001	356	2						
10	43,505	13,264	26	-60.7	.8	.287	-.001	351	3						
10	40,745	12,423	27	-54.4	.8	.319	-.001	347	2						
10	35,930	10,955	20	-42.7	.6	.378	-.001	344	2						
10	31,805	9,697	15	-32.8	.4	.435	+.001	340	2						
10	28,185	8,593	12	-24.4	.4	.488	-.002	336	1						
8.8	24,945	7,604	10	-17.4	.3	.545	0	333	1	336	41	1.0			
8.8	22,055	6,723	20	-11.5	.4	.599	0	329	1	334	0	1.5	0.1		
8.8	19,345	5,898	10	-6.5	.4	.652	-.001	325	1	332	42	0	2.1		
8.8	16,890	5,149	11	-2.1	.4	.706	-.001	322	1	331	-1	44	-1		
8.8	14,595	4,449	7	1.9	.5	.758	-.002	318	0	330	1	50	0	.3.7	.1
8.8	12,470	3,802	10	5.6	.5	.809	-.002	315	0	329	52	-2	4.6	0	
8.8	10,455	3,187	5	9.2	.6	.861	-.001	313	1	330	54	-3	5.7	-1	
8.8	8,575	2,615	6	12.4	.6	.911	-.002	310	1	331	57	-4	7.0	-1	
8.8	6,775	2,066	3	15.5	.9	.964	0	308	1	333	61	-7	8.5	.1	
8.8	5,075	1,548	1	18.3	1.0	1.010	-.003	305	1	336	65	-9	10.3	-.7	
8.8	3,455	1,054	0	21.3	1.1	1.057	-.005	303	1	340	69	-10	12.6	-.8	
8.8	1,925	587	4	23.8	.8	1.104	-.004	301	1	345	76	-5	15.2	-.1	
1000	425	130	-2	26.2	.2	1.151	-.001	299	0	349	81	0	17.7	.1	
1,015	0	0	26.4	.1	1.161	-.001	298	0	349	83	-1	18.3	.1		

The data for the months July–September have been combined into a mean "hurricane season" sounding (table 4). The data are presented in the same form as the mean "hurricane season" sounding for the West Indies area [1] and deviations from the West Indies sounding are shown for all quantities. The "hurricane season" sounding for the West Indies area used data for the months July–October, but October was omitted in preparing the comparable sounding for the Gulf of Mexico area since the intrusion of westerlies at Brownsville and Burrwood is quite evident in the mean temperature data for October. This seasonal change in the circulation patterns is undoubtedly associated with the observed decrease in the frequency of tropical cyclogenesis between September and October [4], a tendency which is more marked in the Gulf of Mexico area than in the West Indies area.

There is little doubt that the "hurricane season" sounding offers a good approximation to normal summer conditions over the northern Gulf of Mexico. The deviations of the station means from the values given in table 4 were nearly all less than 1° C. at lower and middle tropospheric levels and less than 2° C. at all levels. Relative humidity values show more consistent deviations, with Brownsville running 4–5 percent less than the mean at some levels and Havana showing values greater than the means by a similar amount. The stations used in preparing the mean Gulf of Mexico soundings are not distributed so that the data can be considered truly representative of the portions of the Gulf of Mexico where tropical cyclogenesis is most frequent [4]. Data from the Mexican stations at Merida and Veracruz, combined with Burrwood and Brownsville, would probably have led to more representative soundings for the primary hurricane-formation area of the Gulf of Mexico. However, data for Merida and Veracruz—probably because of the shorter length of the records at these stations—were

not included in the tabulations of mean aerological data [2].

The deviations shown in table 4 reveal that differences in the two "hurricane season" soundings are small throughout most of the troposphere. At levels up to 500 mb., the temperature and moisture differences are small enough so that the stability is almost identical over the two areas as revealed by the very small and unorganized differences between the equivalent potential temperature values for the two soundings.³ However, the observed differences indicate that conditions over the Gulf are consistently warmer and drier than in the West Indies area. Deviations of this type in the troposphere are consistent with the fact that easterly flow increases with height over this area in association with the upper tropospheric anti-cyclone located over the southern United States during the summer months [5]. Stratospheric easterlies exist over the whole subtropical area in summer with maximum speeds above the 30-mb. level. The largest temperature differences shown in table 4 appear in the lower stratosphere where the mean easterlies increase most rapidly with height.

The fact that October data are included in the "hurricane season" sounding for the West Indies but not in the similar sounding for the Gulf area has a negligible effect on the features discussed above. This is evident from the fact that the temperature anomalies for the individual months, shown for selected levels in table 5, are very similar to those shown in table 4. The September deviations are smaller than those of the other months, and the vertical distribution is such that the stability over the Gulf, in comparison with the West Indies conditions, is slightly

³ The deviations of equivalent potential temperatures given in table 4 are based on corrected values of the equivalent potential temperatures for the West Indies sounding which appear in a Corrigendum in the *Journal of Meteorology*, vol. 15, No. 6, December 1958, p. 512.

TABLE 5.—Deviation of mean Gulf of Mexico temperature data ($^{\circ}$ C.) from mean West Indies temperature data at selected pressure surfaces for individual months

Pressure (mb.)	July	August	September
50	+1.2	+1.2	+1.5
100	+1.1	+1.8	+.8
150	+1.0	+1.0	+1.1
200	+.8	+.8	+1.0
250	+.8	+.6	+.6
300	+.7	+.5	0
400	+.5	+.3	+.1
500	+.6	+.4	+.4
600	+.7	+.6	+.3
700	+.7	+.6	+.2
800	+1.1	+.9	+.2
900	+1.5	+1.2	+.2
1,000	+.1	+.2	-.4

greater during this month. However, considered over deep layers, differences are less than 1° C.

The fact that differences between the two mean "hurricane season" soundings are small and of such a form as to be consistent with the large-scale climatological features of the area suggests that the mean "hurricane season" sounding presented in [1], although based on data from only three stations, is probably a close approximation to mean conditions over an extensive area in the West Indies-Gulf of Mexico region. Comparison of the mean soundings for individual summer months for the two areas would reveal differences only slightly greater than shown for the "hurricane season" soundings in table 4. This fact, together with the information that synoptic variations are usually small in these areas in the summer months, suggests that these mean soundings may prove much more useful than similar soundings for other areas where the seasonal and geographical gradients, as well as synoptic variability, are much greater. Disturbances—in the form of tropical cyclones which affect most, or all, of the troposphere, and upper-level cyclones which affect the middle and upper troposphere—do occur in the Gulf of Mexico area during the summer months [5]. In the vicinity of these disturbances marked departures from mean conditions can be expected.

4. CLIMATOLOGICAL FEATURES

The mean West Indies data [1] showed that throughout most of the troposphere the warmest mean monthly temperatures are found in September and the coldest values in February. An almost complete reversal was noted in the 200- to 150-mb. layer with the maximum values in February and the minimum values in June-July. In the stratosphere, temperatures were warmest in June-July and coldest in January-February. The temperature data for the Gulf of Mexico area (table 1) show similar variations, except that at levels up to 600 mb. maximum values are observed in August (rather than September) and the reversal in the upper troposphere is first evident at 175 mb. rather than at the 200-mb. level. Also, the transition back to the "normal" seasonal pattern in the stratosphere occurs at a higher level, perhaps reflecting greater mean tropopause heights, with the 100-mb. level lying in the zone of small and somewhat irregular sea-

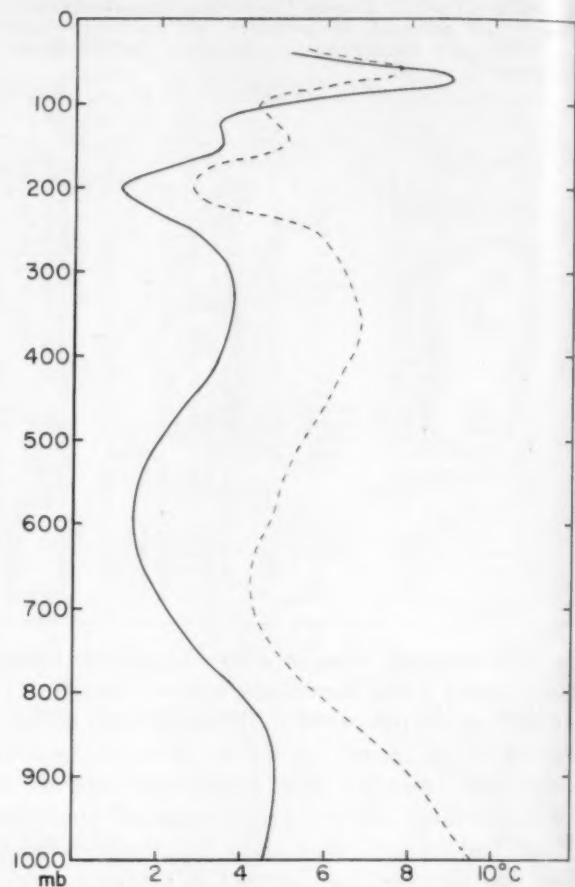


FIGURE 2.—The annual range of the mean monthly temperature for the Gulf of Mexico area (dashed) and the West Indies area (solid).

sonal changes (table 1). The differences in the lower troposphere are consistent with the fact that Burwood and Brownsville are affected by continental influences to a larger degree than the stations used in preparing the mean West Indies soundings. Cold-air outbreaks which are common at these stations during the winter months make the major contribution to the greater range of the mean monthly temperature at lower levels in comparison with those observed in the West Indies data (fig. 2). The magnitude of the range over the Gulf area is greater at all levels in the troposphere; however, the major features of the curves for the two areas are remarkably similar. Minimum values of the range are found in the vicinity of 700-600 mb. and 200 mb., and maximum values near the surface and 350 mb. In the stratosphere, the curves continue to be very similar, with the largest range shown in the West Indies data. The major features shown by this curve have been brought out in other studies [3].

The mean West Indies data showed a marked departure from the normal seasonal trend in early summer with cooling being shown from June to July at tropospheric levels above 700 mb. A similar break in the normal seasonal temperature change is evident in the Gulf data (table 1) but it is weaker and cooling is found only in the 700- and 500-mb. layer.

The mean relative humidity data for the Gulf area were

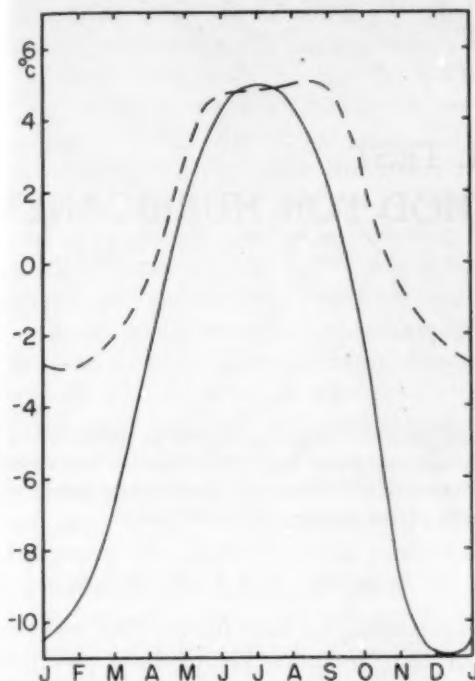


FIGURE 3.—Seasonal course of the Palmén instability index for the Gulf of Mexico area (solid) and West Indies area (dashed).

consistently lower than the mean West Indies values. The maximum deviations were generally in the 900- and 850-mb. layer where, during all months except September, the Gulf values were at least 10 percent less than the West Indies values. During July and August, this relatively dry layer still persisted, but at higher levels the Gulf values were as great as or greater than those for the West Indies area. The low humidities in the 900-800-mb. layer in the summer months, together with the fact that temperature deviations reach a maximum in this vicinity (tables 4, 5), suggest that subsidence is a more prominent feature in this layer over the Gulf of Mexico than over the West Indies area.

It has been pointed out that there are systematic differences between the mean West Indies and Gulf soundings throughout the year, although differences are rather small during the summer months. These two sets of soundings have been studied in relation to the frequency of hurricane formation by computing the Palmén instability index for each area. This index, which Palmén [6] used in his study of climatological aspects of hurricane formation, is defined as the difference between the mean 300-mb. temperature and the temperature of a parcel lifted pseudoadiabatically to this level from the earth's surface. Positive values of the index were considered as a necessary, but not sufficient, condition for hurricane formation.

The Palmén index has been computed for each month of the year using the mean surface and 300-mb. data for the West Indies and Gulf of Mexico areas (fig. 3). The September values in both areas are somewhat lower than those shown by Palmén which attained values of over 9° C. in the Gulf of Mexico area. Similarly, Palmén showed

slightly positive values in the West Indies area in February, while figure 3 shows negative values throughout the winter months. This difference can be accounted for by the fact that Palmén used sea surface temperatures and assumed the surface relative humidity to be 85 percent throughout the whole area considered. He used mean 300-mb. data for September and February from Swan Island. Actually the air temperature is generally slightly lower than the water temperature, and this difference is accentuated in the present case since the mean West Indies and Gulf soundings are based on data taken only at 0300 gmrt. In addition, relative humidity values are less than 85 percent in some months, especially in winter.

The curves of the Palmén index (fig. 3) show a marked seasonal trend which is of the same type in the two areas and which agrees in a qualitative sense with the observed frequency of hurricane formation. Hurricanes are rare during the months which show negative values of the index and a maximum frequency is reached during the months which show positive values. However, the index rises sharply during the spring months and reaches high values in June and July when hurricanes are rare. The index for the Gulf area has already started to fall quite rapidly by September when the maximum of hurricane formation is reached. It is of interest that there are relatively large differences in the value of the index between the two areas in October and November when hurricane formation is still frequent in the West Indies-Caribbean area and much less frequent in the Gulf of Mexico area [4].

Hurricanes form with some regularity in the Gulf of Mexico in October and in the West Indies region in November, although the mean instability index is slightly negative in these areas during these months. However, the hurricane formation periods may well coincide with abnormal periods when the index is positive. Of course, not all features of the seasonal distribution of hurricanes should be expected to fit in with the mean seasonal curves of the simple instability index. The importance of other factors is clearly suggested by the fact that higher values of the index are shown in June-July than in September, although there is a large increase in the frequency of hurricanes between June and September in both areas.

REFERENCES

1. C. L. Jordan, "Mean Soundings for the West Indies Area," *Journal of Meteorology*, vol. 15, No. 1, Feb. 1958, pp. 91-97.
2. B. Ratner, "Upper Air Climatology of the United States. Part I—Averages for Isobaric Surfaces, Height, Temperature, Humidity, and Density," U.S. Weather Bureau *Technical Paper* No. 32, Washington, D.C., 1957.
3. H. Riehl, *Tropical Meteorology*, McGraw-Hill Book Co., Inc., New York, 1954, 392 pp.
4. J. A. Colón, "A Study of Hurricane Tracks for Forecasting Purposes," *Monthly Weather Review*, vol. 81, No. 3, Mar. 1953, pp. 53-66.
5. G. Dean, The 250 mb. Seasonal Wind Circulation Over the Caribbean During 1956-57. (Unpublished.)
6. E. Palmén, "On the Formation and Structure of Tropical Hurricanes," *Geophysica*, vol. 3, 1948, pp. 26-38.

AN OPERATIONAL TEST OF A NUMERICAL PREDICTION METHOD FOR HURRICANES

Lester F. Hubert

U.S. Weather Bureau, Washington, D.C.

[Manuscript received May 25, 1959; revised July 17, 1959]

ABSTRACT

Seventeen forecasts of hurricane tracks, each up to 72 hours, were made by numerical methods under operational conditions as a test of Kasahara's [5] prediction model. Although the small size of the sample precludes making firm conclusions, the results here obtained compare unfavorably with the regularly issued subjective forecasts. In general, the forecast motion is too slow and to the right of the actual hurricane track.

1. INTRODUCTION

The numerical hurricane forecasts described in this report were made to test operationally a prediction model developed by Kasahara [5] at the University of Chicago under a Weather Bureau contract and to test the effect of independent analyses on the forecast. The number of independent analyses available for making duplicate forecasts was, however, unfortunately small.

The fact that this test was made under operational conditions on a "real time" basis enhances its value because there was no possibility that an unconscious bias could be inserted by an analyst who knew the actual hurricane track. Moreover, because the analyses had to be completed by a deadline, they were handicapped by late and missing data in the same manner as the analyses made in hurricane forecast centers, thereby simulating actual operating conditions.

Analyses made by Dr. Riehl at the University of Chicago during his stay at the National Hurricane Research Project, West Palm Beach, Fla., during the 1958 hurricane season were used to produce duplicate forecasts. It so happened that the analysis routine at West Palm Beach produced only three 500-mb. maps for the same time as those made by the writer, so only three comparisons are available. The effect of different analyses is illustrated, but no significant statistics can be derived.

Each hurricane forecast consists of the following steps:

1. Derive graphically the scale and height profile of the hurricane vortex shown on the 500-mb. analysis.
2. Subtract that vortex from the 500-mb. analysis.
3. Produce a stream function field of the 500-mb. surface resulting from step 2 by means of the balance equation routine used by the Joint Numerical Weather Prediction (JNWP) Unit [8].
4. Produce a numerical forecast up to 72 hours on the stream function field from step 3, using the JNWP barotropic-divergent model on the hemispheric octagonal grid [1].
5. Compute a point trajectory starting from the position of the hurricane center on the initial map by use of the hourly forecast fields produced in step 4.

2. METHOD OF ANALYSIS

The 500-mb. analysis used for this test was the machine analysis of the Northern Hemisphere produced by the JNWP automatic data reduction and analysis routine, modified by a reanalysis of the tropical and subtropical Atlantic and Caribbean regions. Figure 1 shows the area that was reanalyzed.

The procedure was to analyze the modification area, perform steps 1 and 2, and substitute the modified analysis (with the vortex removed) into the machine analysis of the octagonal grid, then produce a stream function field (step 3).

Reanalysis was necessary because the region east and northeast of the Antilles is largely devoid of upper-air data and a reliable 500-mb. analysis can be made only by a careful consideration of the surface analysis and the thermal characteristics of tropical atmosphere [4]. While this yields improved analysis within the modification area, it created a problem in making the transition from modi-

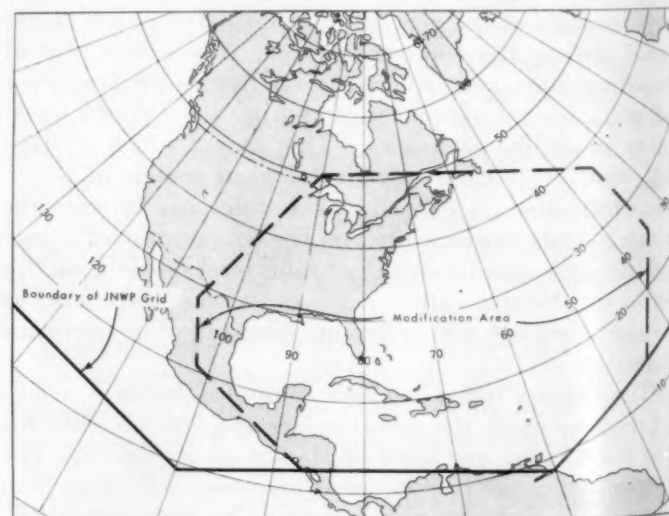


FIGURE 1.—Reanalysis area.

fied to unmodified analysis. At low latitudes especially it was difficult to obtain a smooth transition because the machine analysis frequently produced abnormally low 500-mb. heights on the southern boundaries of the analysis. This was probably due to an error in the analysis routine (corrected shortly after the hurricane season) that extrapolated pressure heights into regions of no data on the basis of erroneous gradients wherever winds were incorporated. Fortunately this error was insignificant at middle latitudes, so the artificial perturbations introduced at the boundaries of the modification area were always in the Tropics and of a small scale; consequently they were quickly smoothed in the forecast routine because waves of less than four grid intervals are not retained.

Hurricane tracks forecast by this method were verified with the official published tracks [9]. Because the official hurricane positions were not available at the time of making the forecasts, several of the initial positions used were different from those that were published, so in order to make a true comparison between forecast and actual motion, the forecast tracks were shifted bodily so that the forecast effectively started from the official initial position. It was necessary to make some adjustment to nine of the forecast tracks; the average adjustment was 34 n.mi.

3. SUMMARY OF FORECAST RESULTS

A total of 17 forecasts was made, each for a 72-hour period. Figures 2-15 show actual and forecast tracks; the errors are tabulated in table 1 and summarized in the polar diagrams, figures 16-20. The polar diagrams show the distribution of forecasts both in a coordinate system pointing in the direction of storm motion and in a system whose orientation remained fixed relative to north. The actual hurricane position at the end of the forecast period is represented by the origin of the diagrams, and the direction of motion is defined as the vector drawn on a polar stereographic map projection from the initial hurricane

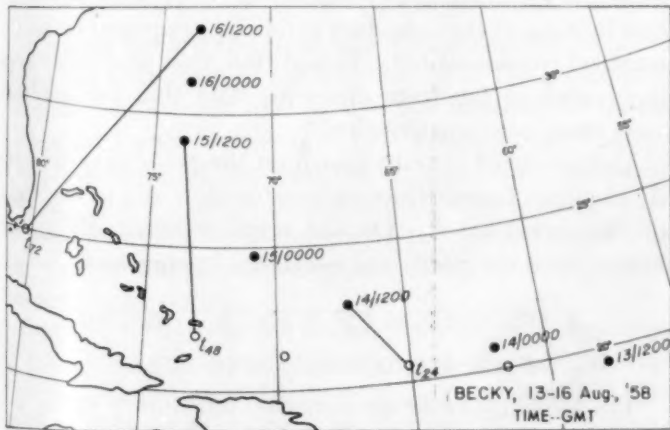


FIGURE 2.—Actual (solid circles) and forecast positions (open circles) for hurricane Becky 1958 for 24 hours (t_{24}), 48 hours (t_{48}), and 72 hours (t_{72}) from position at 1200 GMT, August 13. Lines connect corresponding forecast and actual positions.

TABLE 1.—Errors in forecast hurricane tracks

Storm	Code on figs. 16-19	Date (1200 GMT)	Forecast error (n. mi.)		
			24 hr.	48 hr.	72 hr.
A. FORECASTS MADE FOR OPERATIONAL TEST					
(Becky)*	B-1	13 August 1958	(183)	(427)	(620)
Becky	B-2	14 August 1958	232	356	938
(Cleo)	C-1	15 August 1958	(400)	(765)	(902)
Cleo	C-2	16 August 1958	(378)	(618)	(1,120)
Daisy	C-3	17 August 1958	117	133	369
Daisy	D-1	25 August 1958	233	393	636
Daisy	D-2	26 August 1958	30	143	418
Daisy	D-3	27 August 1958	109	313	404
Daisy	D-4	28 August 1958	107	209	235
Ella	E-1	1 September 1958	194	364	684
Ella	E-2	2 September 1958	52	212	502
Ella	E-3	4 September 1958	193	399	—
Fifi	F-1	7 September 1958	201	381	585
Fifi	F-2	8 September 1958	154	378	778
Average error			147	274	564
B. FORECASTS MADE FROM INDEPENDENT ANALYSIS					
Becky	B-2	14 August 1958	316	524	1,320
Ella	E-1	1 September 1958	157	238	244
Fifi	F-1	7 September 1958	88	233	468

*Forecasts indicated by parentheses not included in average error figure shown here or in "center of gravity," figs. 16-19.

position to the position at the end of the appropriate forecast period.

Each diagram also shows a "center of gravity" of the forecast distribution, but it should be noted that these

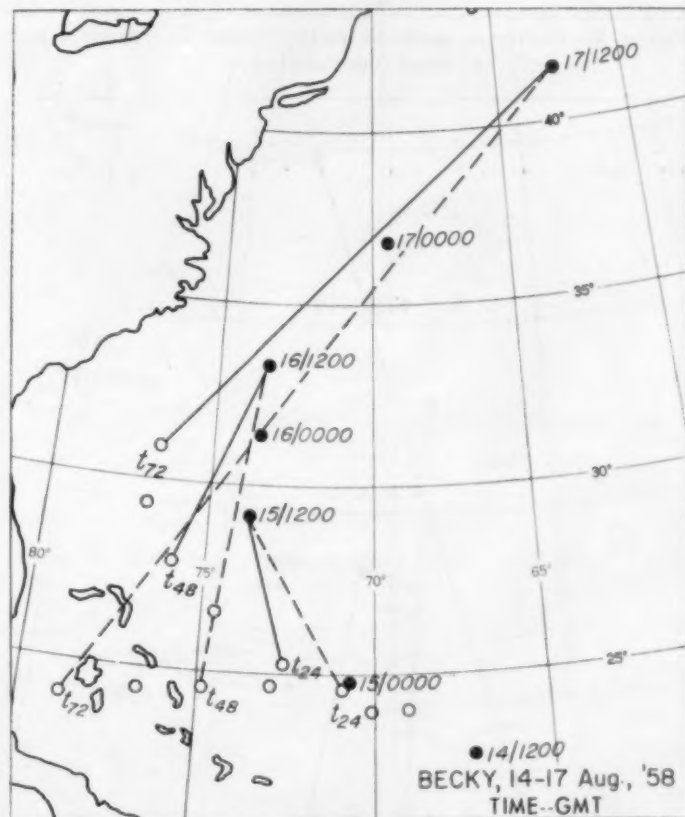


FIGURE 3.—Actual (solid circles) and forecast positions (open circles) for hurricane Becky 1958 from 1200 GMT August 14. Actual position is connected to test forecast position by solid line, to position forecast from independent analysis by dashed line.

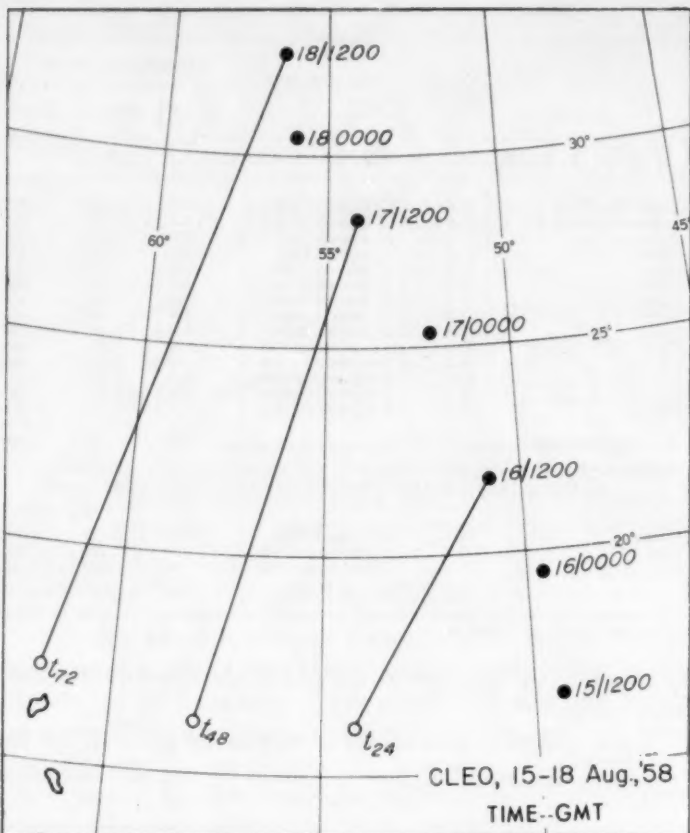


FIGURE 4.—Hurricane positions (solid circles) and forecast positions (open circles).

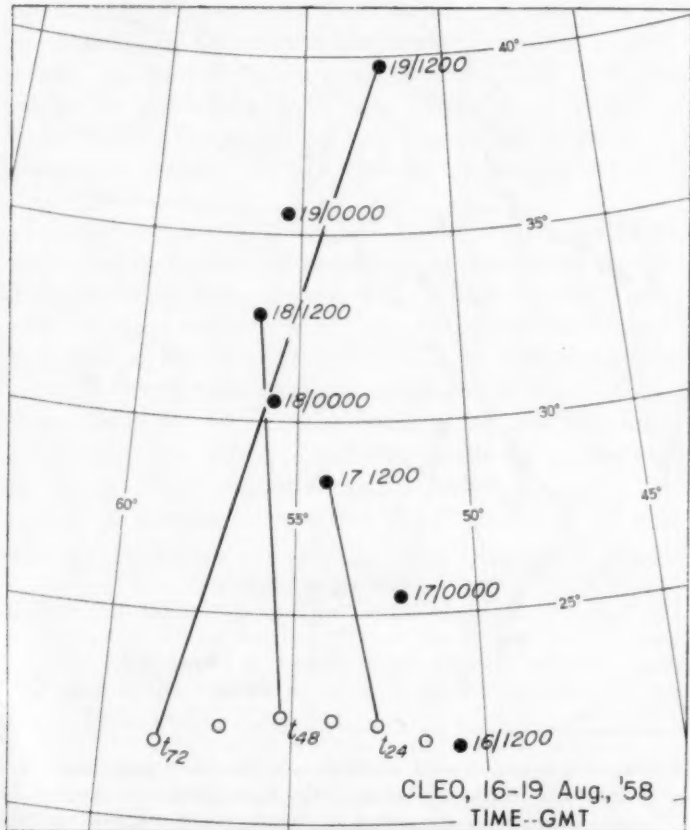


FIGURE 5.—Hurricane positions (solid circles) and forecast positions (open circles).

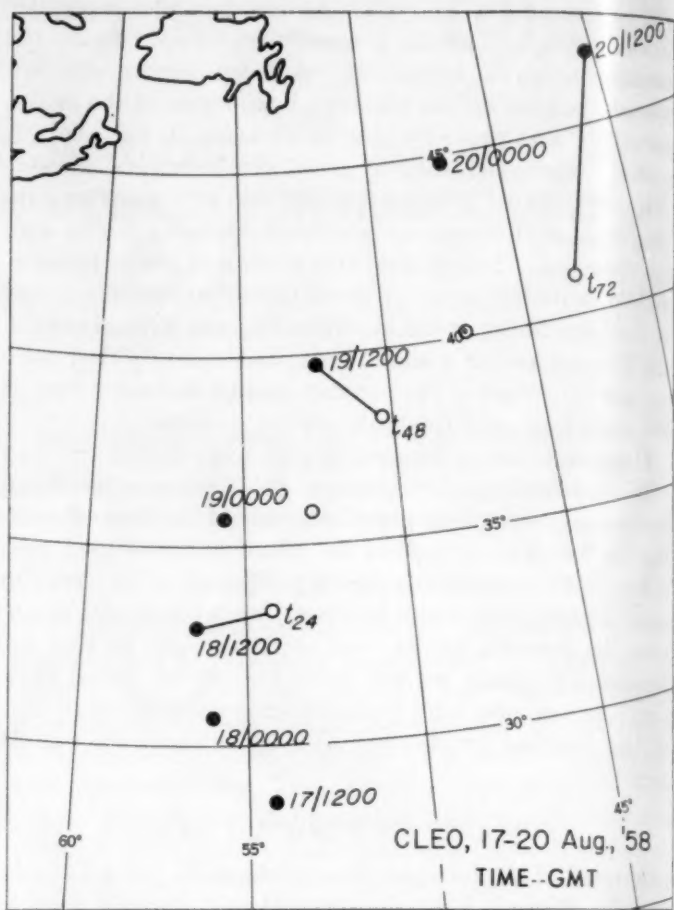


FIGURE 6.—Hurricane positions (solid circles) and forecast positions (open circles).

statistics refer to but 11 of the forecasts. Three forecasts based on Dr. Riehl's analyses were considered as a separate sample. In addition, three "real time" forecasts—Becky, 13 August; Cleo, 15 August; and Cleo, 16 August 1958—were omitted from verification statistics because the area in which they moved during the forecast period was quite near the boundary of the computation grid. As a consequence, the field of motion was not realistically forecast because of the boundary conditions required by mathematical considerations. In addition, that particular area is situated so far from upper-air data that the analyses were open to serious question.

The center of gravity shown on the polar diagrams indicates that forecast motion was too slow and to the right of the actual track. On the north-oriented diagram a bias toward the north and northeast is suggested.

4. DISCUSSION OF FORECAST RESULTS

ERROR ALONG DIRECTION OF MOTION

The tendency to forecast motion too slow is partly due to truncation error, a shortcoming of the numerical procedure of using finite difference quotients as an estimate of derivatives which was discussed in an earlier experiment [3], but in the present model the vortex subtraction



FIGURE 7.—Hurricane positions (solid circles) and forecast positions (open circles).

adds another possible source of speed bias. When the hurricane lies near a col the effect of subtracting the vortex is to produce an extremely flat gradient right at the point where the trajectory starts.

At this stage the method of smoothing the residual flow field is critical. Because the large-scale forecast with the barotropic model does not change details of this nature very rapidly, the initial gradient usually persists for many hours in the forecast field so that the storm displacement is largely dependent upon the initial conditions.

ERROR TO RIGHT OF DIRECTION OF MOTION

The bias toward the right might be due either to a tendency for hurricanes to move to the left of the geostrophic wind at the 500-mb. level or to a systematic error in the numerical forecast procedure that produced the bias toward the right of the geostrophic wind. In this small sample with the great dispersion of forecast errors it is of course impossible to determine the cause for the bias, but certain indications do appear that yield insight into the sources of error.

Concerning the possible tendency for hurricanes to move to the right of the geostrophic wind at the 500-mb. level, there is no indication in other work on the subject that such a tendency exists (e.g., see [6] and [7]). As a consequence, it is reasonable to examine the forecast routine for the probable cause.

To begin with, it should be noticed that the direction of the storm forecast in this test was generally toward



FIGURE 8.—Hurricane positions (solid circles) and forecast positions (open circles).

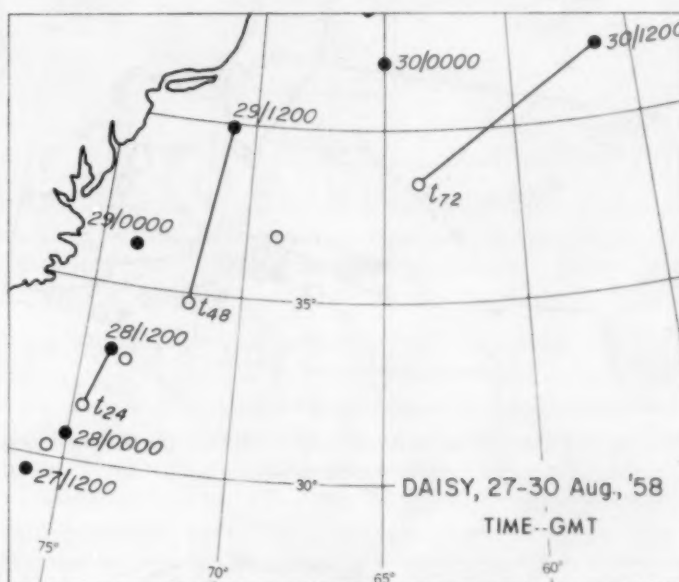


FIGURE 9.—Hurricane positions (solid circles) and forecast positions (open circles).



FIGURE 10.—Hurricane positions (solid circles) and forecast positions (open circles).

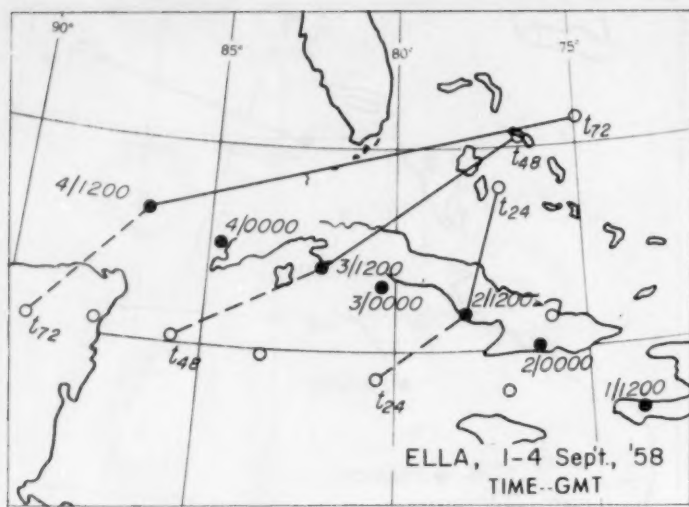


FIGURE 11.—Hurricane positions (solid circles) and forecast positions (open circles). Actual position is connected to test forecast position by solid line, to position forecast from independent analysis by dashed line.

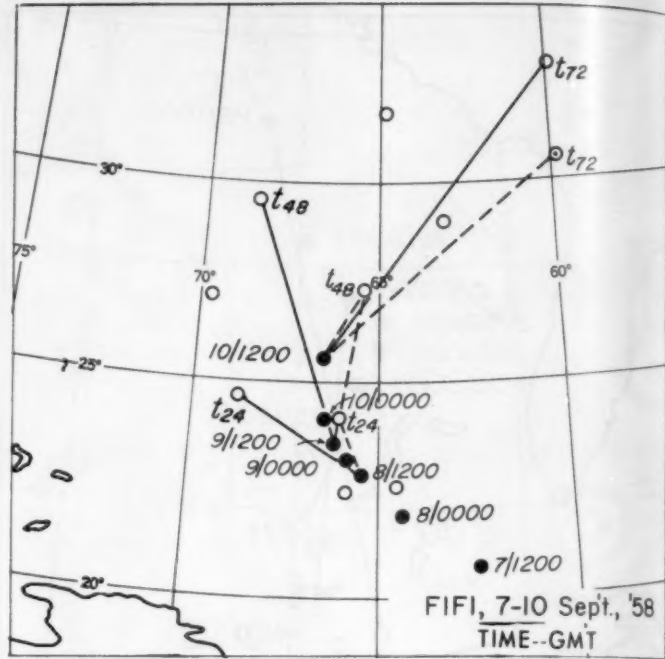


FIGURE 14.—Hurricane positions (solid circles) and forecast positions (open circles). Actual position is connected to test forecast position by solid line, to position forecast from independent analysis by dashed line.

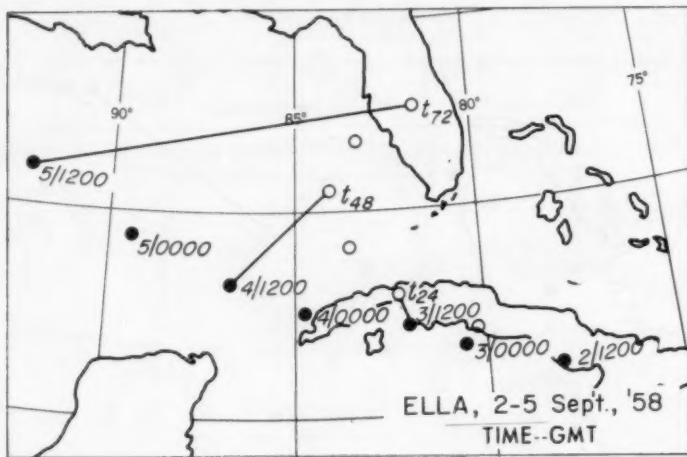


FIGURE 12.—Hurricane positions (solid circles) and forecast positions (open circles).

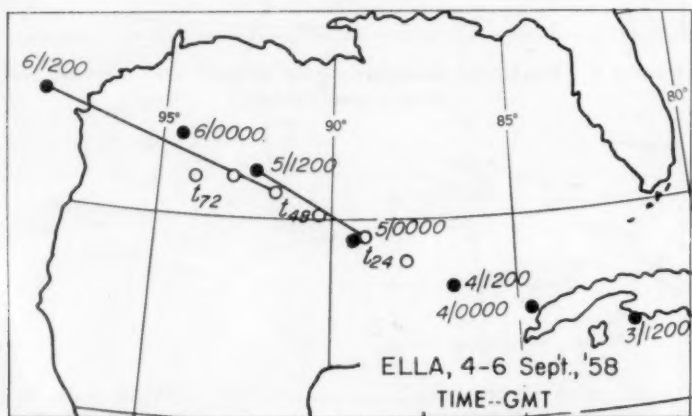


FIGURE 13.—Hurricane positions (solid circles) and forecast positions (open circles).

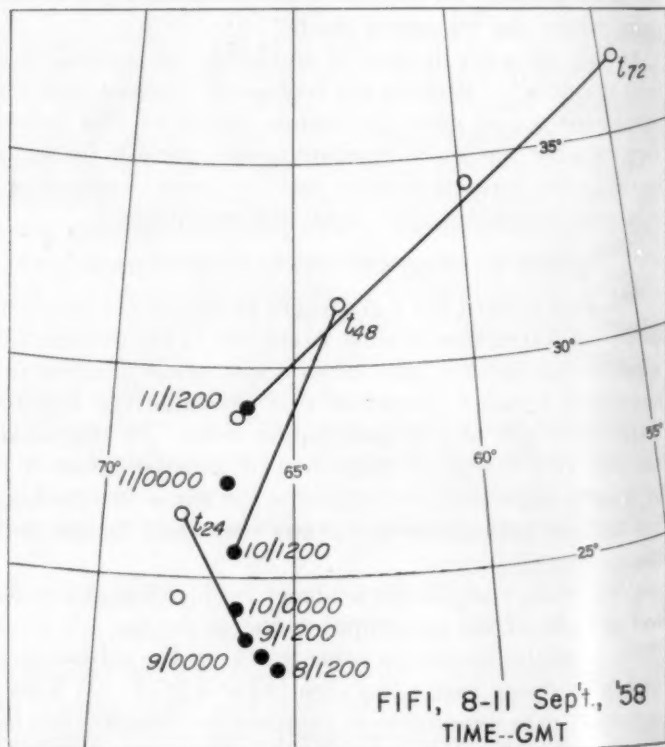


FIGURE 15.—Hurricane positions (solid circles) and forecast positions (open circles).

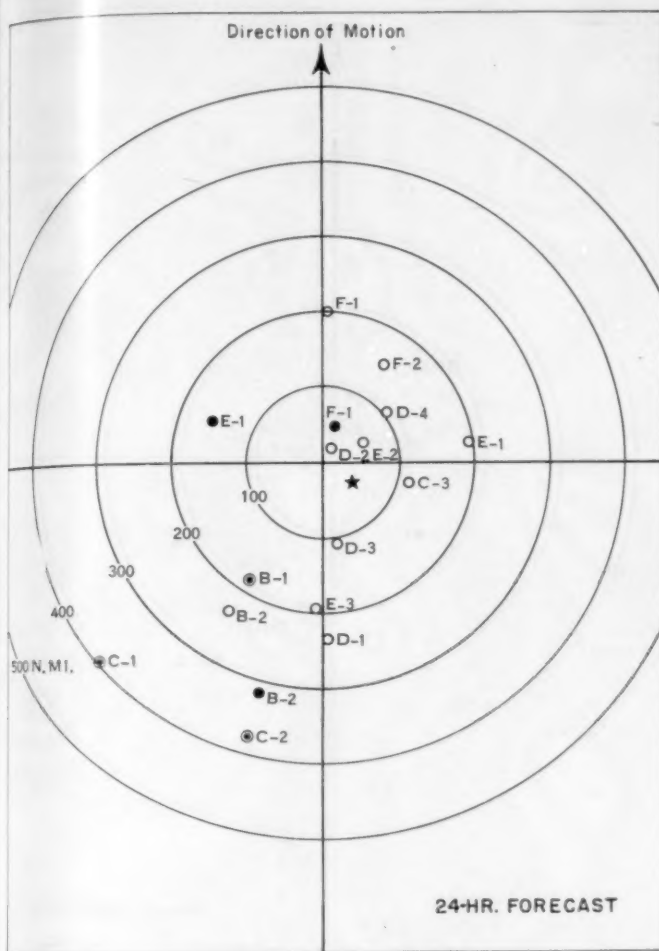


FIGURE 16.—Distribution of 24-hour forecasts relative to direction of motion. Star marks centroid. Storm identifiers listed in table 1.

the northwest so that a bias to the right of the true track would also show up as a bias toward the east. Now if a systematic error in the trajectory computations produced the bias, it would arise because of the systematic influence of a residual trough left by the vortex subtraction or through the vortex interaction term in the trajectory equations. Examination of the forecast stream function fields showed that the bias was not due to a residual trough; therefore the effects of the trajectory computations were examined.

Trajectories are computed in step 5 of the forecast procedure by application of:

$$C_x = -a \frac{\partial \psi}{\partial y} - K \frac{\partial \eta}{\partial y} \quad (1)$$

$$C_y = a \frac{\partial \psi}{\partial x} - K \frac{\partial \eta}{\partial x} \quad (2)$$

C_x =trajectory speed along the x -axis

C_y =trajectory speed along the y -axis

ψ =stream function

η =absolute vorticity ($f + \zeta = \eta$) where ζ is the relative vorticity and f the Coriolis parameter

a =a constant for scaling to proper units

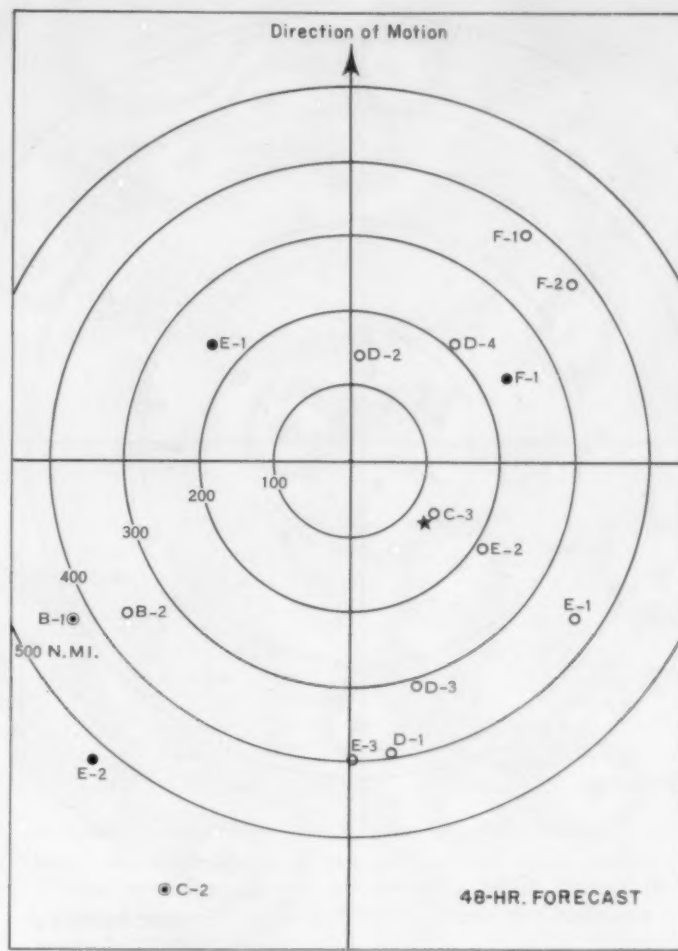


FIGURE 17.—Distribution of 48-hour forecasts relative to direction of motion. Star marks centroid for open circles. Storm identifiers listed in table 1.

K =a number obtained from the hurricane profile on the 500-mb. surface to represent the magnitude of the vortex (contains the appropriate scale factor a)

The first terms on the right side of equations (1) and (2) are the geostrophic wind components in the stream function field, while the last terms, depending upon the size of the hurricane vortex (K) and the gradient of absolute vorticity ($\Delta\eta$), are the vortex interaction terms.¹

Now in this particular model a symmetric vortex is removed (step 2) so that the residual relative vorticity is a measure of the asymmetry about the storm. Since there is no gradient of Coriolis force in an east-west direction, it is only asymmetry in the east-west direction that can produce a north-south component of storm motion. On the other hand, the east-west component contributed by this term depends upon the asymmetry along a north-south axis combined with the north-south gradient of Coriolis force. It is therefore of interest to estimate the magnitude of the interaction term in these cases and to determine whether the contribution was in the correct direction.

¹ It will be noticed that this "interaction" term is actually unilateral, for the 500-mb. field influences the hurricane trajectory, but the vortex, having been removed before the forecast starts, can have no effect on the 500-mb. field.

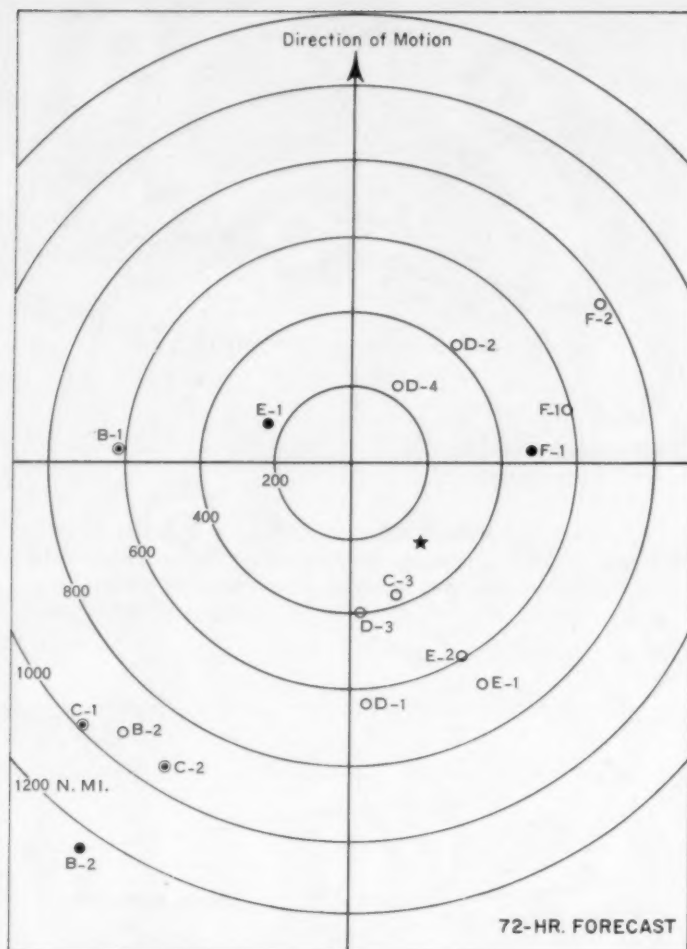


FIGURE 18.—Distribution of 72-hour forecasts relative to direction of motion. Star marks centroid for open circles. Storm identifiers listed in table 1.

On the basis of figures 19 and 20, which show a bias toward the east, indications are that the effect of the Coriolis term in the trajectory equations is in the proper direction, for without it the error would have been even greater toward the east.

In an effort to make some quantitative estimate of the effect, two different trajectory computations were made on four storms; the first trajectory by the procedures outlined above and a second computation following the same routine except that the vortex interaction term was eliminated so that the motion was entirely due to the "balanced" wind. The differences between these trajectories are tabulated in table 2. Where the effect of the vortex term and the forecast error have opposite signs, the effect of the term was to reduce the error; where the signs are the same, the effect was to increase the error. The underlined items are the cases where the effect was favorable.

First, it is clear that the contribution of the Coriolis term to the absolute vorticity gradient is a prominent effect for the signs in the third column are all negative (displacement to the west). Since the signs in the fourth column are a function of the relative vorticity gradient only, there is an indication that the gradient of relative

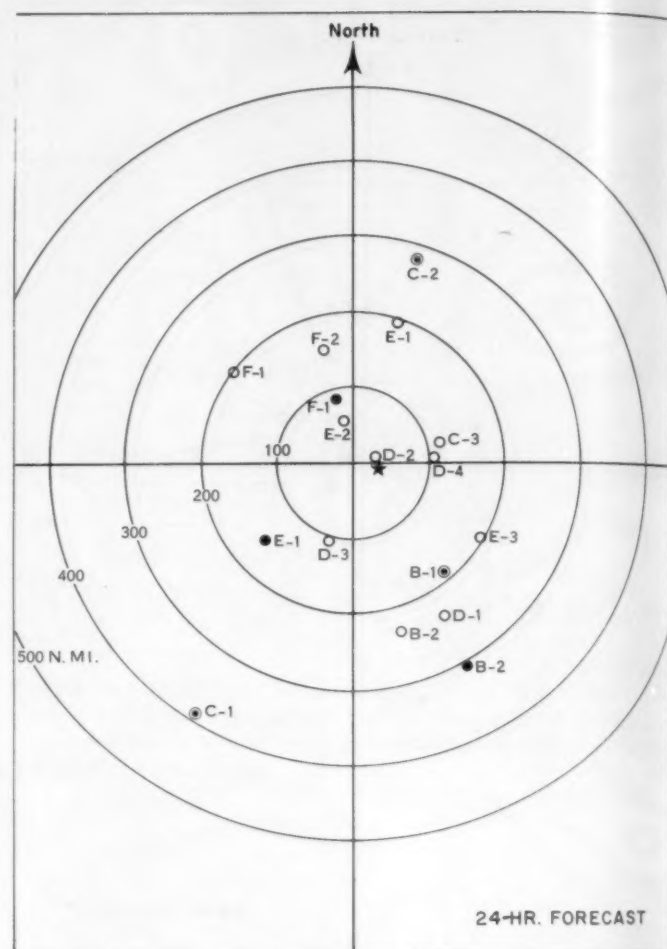


FIGURE 19.—Distribution of 24-hour forecasts relative to north. Star marks centroid for open circles. Storm identifiers listed in table 1.

vorticity in an east-west direction is generally smaller than the gradient of Coriolis force in the north-south direction—an indication of the small asymmetry in the cases tested.

Second, the overall influence of this term has been beneficial for there are more favorable cases than unfavorable.

Third, the most definitive result is the indication that the influence of the vortex term in this model is insignificantly small for storms of the size tested for it contributes displacement in 24 hours that is less than the uncertainty in hurricane position.

TABLE 2.—Forecast error compared to effect of vortex interaction term (in units of grid lengths, 381 km. at 60°)

Storm and forecast	Vortex scale, K (km.)	Effect of vortex interaction term—		24-hour forecast error—	
		To east	To north	To east	To north
Daisy-1	200	-0.05	-0.03	0.05	0.20
Ella-3	210	<u>-0.07</u>	0.02	0.40	-0.40
Fif-1	150	<u>-0.03</u>	<u>0.00</u>	-1.30	1.00
Fif-2	125	-0.02	-0.02	-0.05	0.75

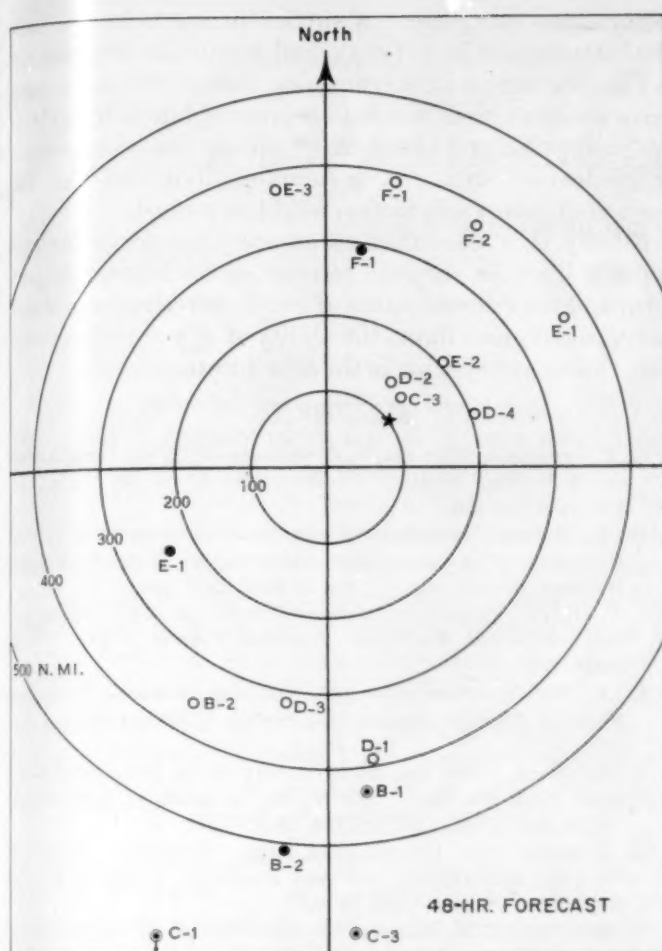


FIGURE 20.—Distribution of 48-hour forecasts relative to north. Star marks centroid for open circles. Storm identifiers listed in table 1.

5. ERROR IN FORECASTING LARGE-SCALE FEATURES

The error in hurricane trajectory forecasts that was contributed by inaccuracies of the numerical weather prediction model in predicting large-scale features was investigated by computing trajectories on observed rather than on forecast stream function fields. This was possible of course only where forecast steps 1, 2, and 3 had been completed on successive days, a requirement which limited the sample to five cases of 24-hour forecasts. Figure 21 illustrates the results that would have been realized if the large-scale pattern had been "perfectly" forecast; that is, if the forecast valid 24 hours after the initial time had been exactly the same as the stream function map obtained from analysis of the actual data 24 hours after the initial map. This polar diagram shows both the forecast positions and the positions computed from a "perfect forecast," as well as the centers of gravity. The average error for those five forecasts was 118 n. mi. in 24 hours; the "perfect large-scale forecast" would have given an average error of 74 n. mi.—an improvement of 44 n. mi.²

²The error of 74 n. mi. that occurs despite a "perfect large-scale forecast" is in part a reflection of the fact that the analysis of actual data includes a certain degree of uncertainty and thus does not actually represent a perfect forecast.

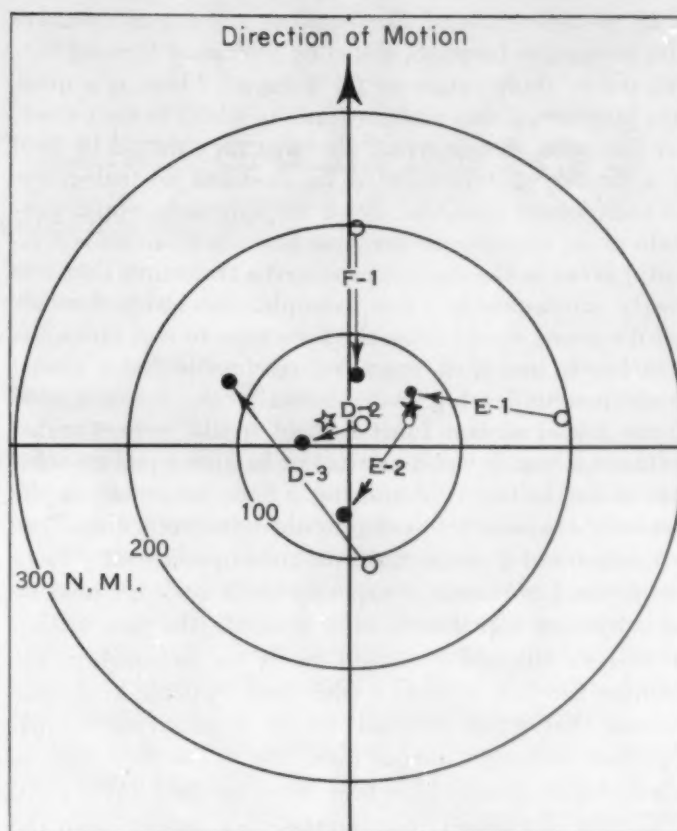


FIGURE 21.—Distribution of 24-hour forecasts (open circles) and 24-hour motion computed on observed stream function fields (solid circles) for the same period. Respective centroids indicated by stars.

Another source of error that is peculiar to this method concerns the solution of the balance equation in regions of a flat gradient such as sometimes results from subtracting the hurricane vortex. This is illustrated by the Daisy forecast of 25 August (fig. 7). Minor features in the flat height field produced a small anticyclone in the stream function field which in turn produced a forecast trajectory that spiraled to the south while the hurricane actually drifted northward. It is not obvious from inspection of the 500-mb. height field just what the balance equation solution will produce insofar as these minor features are concerned, and it sometimes turns out that features quite unimportant to the large-scale forecast produce a minor eddy which can then dominate the point trajectory.

In summary, it appears that a significant part of the error is due to shortcomings of the numerical model in predicting the large-scale pattern, but that *uncertainty in the analysis due to sparse data is an equally serious source of error* quite apart from the method of hurricane track forecasting applied.

6. CONCLUSIONS

A comparison of the results reported here with various verification statistics on subjective hurricane forecasts reveals that numerical hurricane forecasts by this model

in its present state of development are not competitive with subjective forecasts issued by hurricane forecast centers, either short range or for 3 days. There is a question, however, if this is the manner in which to use numerical forecasts of this type. Perhaps they should be used as a frame of reference to be modified by subjective methods where possible. Such an approach would preclude using this type of machine forecast when some accidental event in the routine produced a trajectory that was clearly unreasonable. For example, the Daisy forecast just discussed would cause the forecaster to reexamine the situation to see if it appeared reasonable for a closed anticyclone to develop in the critical area. Examination of the initial stream function field would have revealed in this case that it was a product of balance equation solution of the initial field and not a forecast at all, so the southerly trajectory forecast would have been discarded.

A numerical forecast that would be operationally more useful could of course incorporate the knowledge used by the subjective forecasters. For example, the past motion as well as climatology could easily be included in the machine forecast to yield a combined dynamic-kinematic forecast that would take advantage of empirical knowledge that serves the human forecaster. The first steps in this direction already have been taken by the JNWP Unit. A method developed incorporates past motion into the analysis, and the hurricane forecasts for the 1959 season are expected to show the resulting improvement.

Conclusions based on such a small sample are not justified, but the various indications resulting from this analysis point to aspects of this scheme that should receive additional study.

Because the balance equation can produce minor features that do not harm the large-scale forecast but that can be disastrous to a point trajectory, some space smoothing of the stream function field is mandatory before tra-

jectories are computed. A surface-fitting technique such as that reported in [2] may well serve this function.

The subtraction of a symmetric vortex does not always leave a smooth basic flow field because of initial irregularities in the analysis—some of which are due to inaccurate or inadequate data. It is therefore indicated that the method of vortex subtraction might be revised.

Finally it is clear that an accurate hurricane forecast depends upon an accurate forecast of the large-scale pattern, and the current status of our upper-air observations in oceanic regions limits the ability of any model to eliminate this source of error in the near future.

REFERENCES

1. G. P. Cressman, "Barotropic Divergence and Very Long Atmospheric Waves," *Monthly Weather Review*, vol. 86, No. 8, Aug. 1958, pp. 293-297.
2. W. E. Hubert, "Hurricane Trajectory Forecasts from a Non-Divergent, Non-Geostrophic, Barotropic Model," *Monthly Weather Review*, vol. 85, No. 3, Mar. 1957, pp. 83-87.
3. L. F. Hubert, "Numerical Weather Prediction of Hurricane Motion," *National Hurricane Research Project Report No. 2*, July 1956.
4. L. F. Hubert, "Analysis Aids for the American Tropics," *Monthly Weather Review*, vol. 86, No. 6, June 1958, pp. 201-218.
5. A. Kasahara, "The Numerical Prediction of Hurricane Movement With the Barotropic Model," *Journal of Meteorology*, vol. 14, No. 5, Oct. 1957, pp. 386-402.
6. B. I. Miller, "The Use of Mean Layer Winds as a Hurricane Steering Mechanism," *National Hurricane Research Project Report No. 18*, June 1958, 24 pp.
7. H. Riehl and N. M. Burgner, "Further Studies of the Movement and Formation of Hurricanes and Their Forecasting," *Bulletin of the American Meteorological Society*, vol. 31, No. 7, Sept. 1950, pp. 244-253.
8. F. G. Shuman, "Numerical Methods in Weather Prediction: I. The Balance Equation," *Monthly Weather Review*, vol. 85, No. 10, Oct. 1957, pp. 329-332.
9. Staff, Weather Bureau Office, Miami, Fla., "The Hurricane Season of 1958," *Monthly Weather Review*, vol. 86, No. 12, Dec. 1958, pp. 477-485.

CORRECTION

Vol. 87, April 1959, p. 133: In figure 4, $\Delta T/\Delta t$ should be -0.8° C. at 425 mb. and -1.2° C. at 475 mb.

P. 134: In figure 5, $\Delta T/\Delta t$ should be -0.8° C. at 475 mb. and -1.4° C. at 625 mb.

THE WEATHER AND CIRCULATION OF JUNE 1959

A Month With an Unusual Blocking Wave

Raymond A. Green

Extended Forecast Section, U.S. Weather Bureau, Washington, D.C.

1. INTRODUCTION

Extensive blocking during the latter half of June 1959 culminated in the second lowest 5-day mean zonal index of record for June. The major blocking activity of the month had little effect in western North America, but led to substantially reduced temperature anomalies in the eastern United States where temperatures had been much above normal in May [1]. Conversely, the cold temperatures and strong mean trough over the Western States in May were replaced by predominantly much above normal temperatures and mean ridge conditions in June. Reversals of this type have been more frequent from April to May [2], though a strong May-June reversal occurred in 1955 [3].

2. GENERAL CIRCULATION

Features of the mean 700-mb. circulation (fig. 1) characteristic of blocking were the out-of-phase, "shattered" nature of mean troughs and their irregular spacing around the hemisphere. The one continuous full-latitude trough over eastern Canada and the western Atlantic was strongly distorted by the supernormal half wavelength upstream associated with confluence over southern Canada. Over the oceans at middle latitudes the mean troughs were spaced rather closely, with the blocking character of the ridges between them best revealed in the height anomaly field.

Magnitudes of the mean monthly anomaly centers were remarkably large, in view of the tremendous height changes that occurred within the month (fig. 2C). Some of the changes occurred near rather strong monthly mean centers of anomaly at high latitudes. Intensity of the strongest height anomaly center over northern Siberia varied little, but centers over the Aleutians and the Canadian Arctic, prominent in figure 1, did not appear in the mean of the first half-month (fig. 2A). While these centers were not associated with separate Highs in the monthly mean height field (fig. 1), they were related to the split Aleutian Low and the westward displacement (from normal) of the mean Low over Canada. The Arctic Low was stronger than normal, displaced toward Spitsbergen, and remained relatively unchanged through the month.

The greatest change from May (fig. 3) took place over northern Siberia, where a strong ridge displaced a deep mean trough (see fig. 1 of [1]). Downstream the Asiatic

coastal trough deepened, forcing eastward the Pacific trough and a lobe of the Aleutian Low. This accounted for extensive falls in the eastern Pacific, where a strong mean ridge had dominated the May pattern. Changes downstream over the United States were smaller but sufficient to reverse almost completely the field of 700-mb. height anomaly. During this reversal general rises occurred over the Western States early in June, but the falls over the Eastern States were mainly reactions to blocking after midmonth. Negative anomalies over the Gulf States were associated with remnants of tropical storms Arlene and Beulah and two weaker tropical depressions.

Other information about the circulation can be gleaned from the mean monthly wind field at 700 mb. (fig. 4). The mean jet maximum was well defined and stronger than normal over the eastern Pacific and the eastern Atlantic. The mean jet followed the normal path rather closely over the oceans, but was located north of normal over North America. This is further indication that blocking tended to bypass the North American Continent.

The zonal index (fig. 5) underwent a complete oscillation, continuing the series of index cycles dating back to April 1959 [4]. In June the excess of zonal westerlies over normal during the first half of the month was nearly balanced by a deficit during the second half, so that the average for the month was about normal. Similar compensation occurred at most latitudes of the western sector of the Northern Hemisphere, and departures from the normal 700-mb. windspeed profile (not shown) were small.

3. BLOCKING

While blocking persisted throughout the month over Asia, its effects were negligible in the western sector of the hemisphere until after midmonth. In the first half-month (fig. 2A) the strongest anomaly centers in the western sector of the hemisphere were negative and located at middle or high latitudes. With the advent of blocking, the picture changed radically during the second 15-day period, and the negative centers were all but obliterated in the northern Pacific. A huge area of positive anomaly centered near the Aleutians became dominant there (fig. 2B), and extensions of this positive area through other strong centers in the Beaufort Sea and Baffin Bay completed an anticyclonic pattern of remarkable proportions at high latitudes in the western part of the hemisphere.

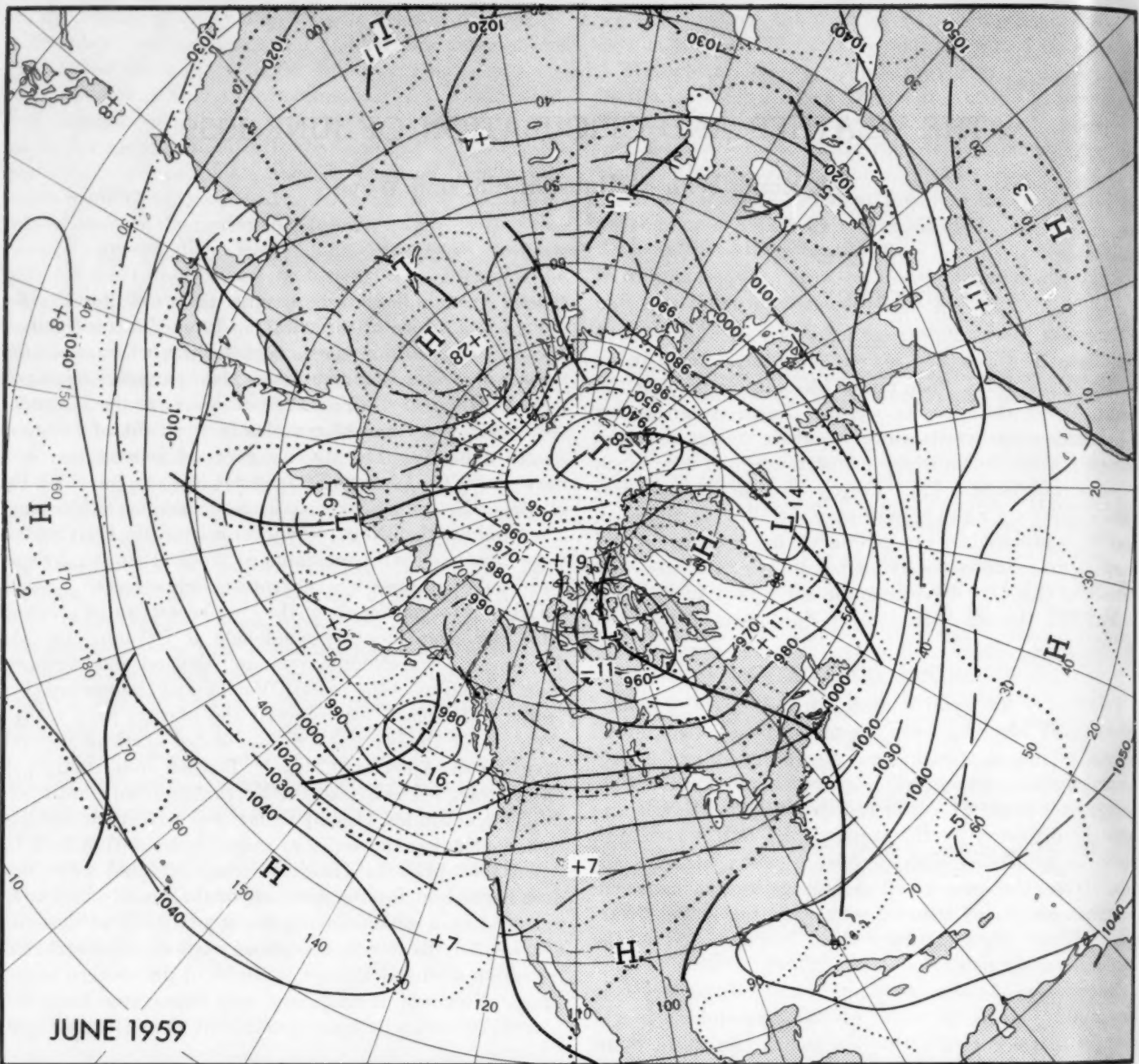


FIGURE 1.—Mean 700-mb. contours (solid) and height departures from normal (dotted), both in tens of feet, for June 1959. Blocking activity was marked in the area of positive anomaly around the northern boundary of North America from Newfoundland to southwestern Alaska.

The depressed negative centers over the Atlantic Ocean were arrayed in the "omega" pattern often observed with blocking.

Figure 6 displays a series of 5-day mean maps for periods chosen to represent the circulation by weeks. The incipient stage of a blocking wave appeared the first week (June 2-6, fig. 6A) over northwestern Russia. During this period the zonal index was high (fig. 5) in the western sector of the hemisphere, and amplitudes of waves in the strong westerly flow were small. During the same period a High just northwest of Greenland was associated with a positive anomaly of about 100 feet.

During the subsequent week, blocking spread to the Atlantic ridge, and the positive anomaly near Greenland moved southward to Hudson Bay and became more intense. The ridge in the northern Pacific pushed strongly northward, so that by June 9-13 (fig. 6B) the zonal index had been reduced to just about normal.

Thereafter the Atlantic ridge built sharply, spreading westward, to the Maritime Provinces. As positive anomalies bridged westward, the anomaly center in Hudson Bay grew in size and intensity and shifted to the Beaufort Sea. This center had joined across Alaska to the northern Pacific High by June 16-20 (fig. 6C). At this

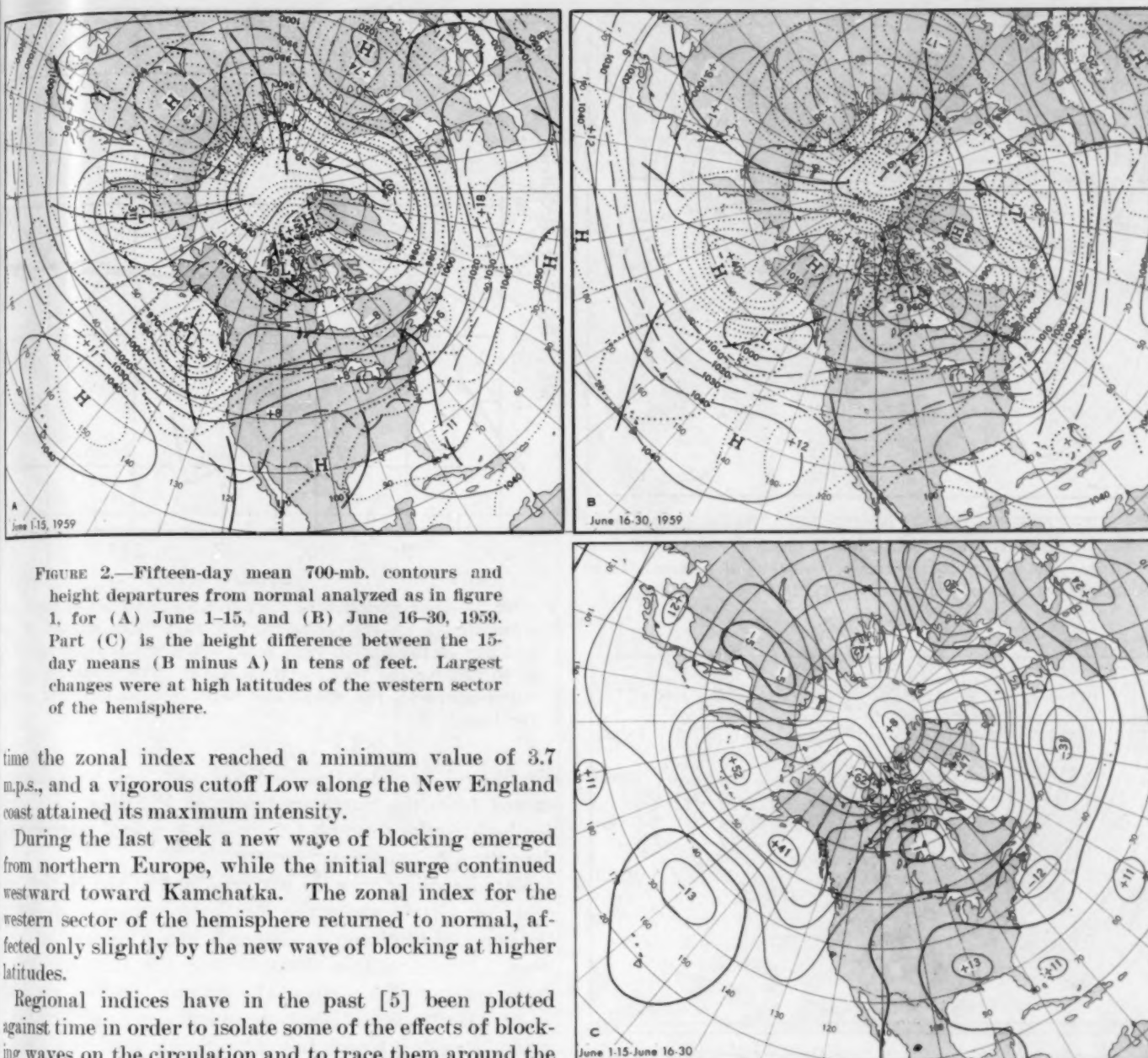


FIGURE 2.—Fifteen-day mean 700-mb. contours and height departures from normal analyzed as in figure 1, for (A) June 1-15, and (B) June 16-30, 1959. Part (C) is the height difference between the 15-day means (B minus A) in tens of feet. Largest changes were at high latitudes of the western sector of the hemisphere.

time the zonal index reached a minimum value of 3.7 m.p.s., and a vigorous cutoff Low along the New England coast attained its maximum intensity.

During the last week a new wave of blocking emerged from northern Europe, while the initial surge continued westward toward Kamchatka. The zonal index for the western sector of the hemisphere returned to normal, affected only slightly by the new wave of blocking at higher latitudes.

Regional indices have in the past [5] been plotted against time in order to isolate some of the effects of blocking waves on the circulation and to trace them around the hemisphere. The progress of a blocking surge from the eastern Atlantic to the northern Pacific is shown in figure 8. The wave moved rapidly upstream, affecting adjacent 80° zones at subsequent intervals of 3 or 4 days. It is interesting to note the extent to which the disturbance affected index values of different zones. For instance, the reaction was much greater over the oceans than over continental North America or Asia. This behavior is difficult to explain but may have been related to the eccentric location of the semipermanent Arctic Low and the strong High over Siberia.

4. TEMPERATURES

It has been noted that the monthly temperature anomaly pattern over the United States (fig. 9) strongly reflected the circulation reversal from May to June. Only 40 percent persistence (0+1 classes) was observed, much

less than the 70 percent expected [2]. A reversal in 1955 [3] resulted in even less persistence, 35 percent, from May to June.

The anomaly pattern for May 1959 favored baroclinic development, with vigorous storms advecting cool air behind them along the frontal boundary separating cool air in the North and West from warm air in the East and South. Just the opposite is indicated in the pattern for June, when the boundary was also oriented southwest-northeast but separated warm air in the Northwest, from cool air in the Southeast. This and the precipitation pattern suggest that limited insolation due to cloudiness was more responsible for cool anomalies in June than advected cool air.

Abnormal warmth in the Southwest was attended by high percentages of possible sunshine, and new records

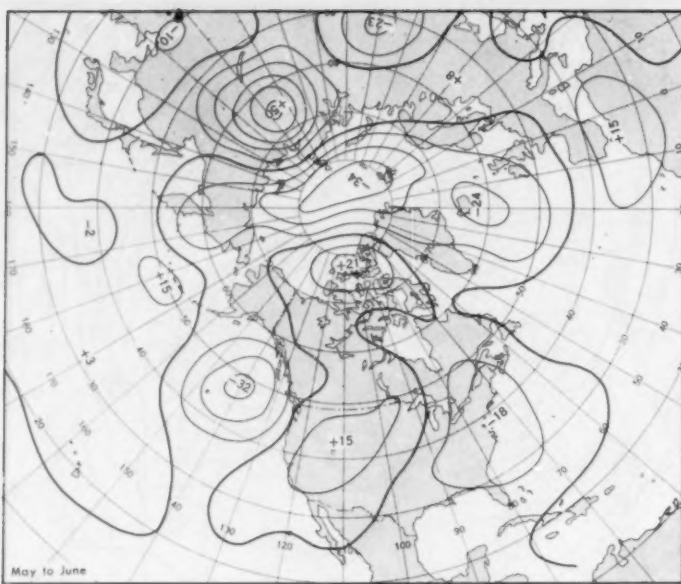


FIGURE 3.—Difference between monthly mean 700-mb. height anomalies for May and June 1959 (June minus May) in tens of feet. Changes over the United States accompanied a reversal of the temperature anomaly pattern from May to June.

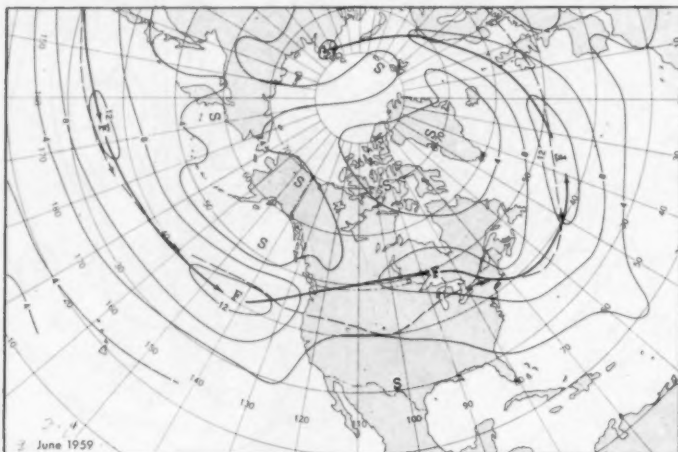


FIGURE 4.—Mean 700-mb. isotachs in meters per second for June 1959. Solid arrows indicate principal axes of mean winds and dashed arrows their normal June positions. Over the Pacific and Atlantic the axes followed closely the normal path, but northward displacement was evident over North America.

were established for both. Sacramento, Calif., reported 100 percent of possible sunshine. Ely, Nev., had new records for possible sunshine and highest average temperature. Las Vegas, Nev., Los Angeles Airport, Calif., and Yuma, Ariz., all had record high temperatures for June.

Temperature anomalies [6] for the weeks corresponding to the 5-day periods in figure 6 are shown in figure 7. The pattern for the first week was typical of that associated with a high index circulation. Warmer than normal temperatures prevailed over the West and North, and cooler than normal over the Southeast. There were relatively small changes during the second week, as some cool

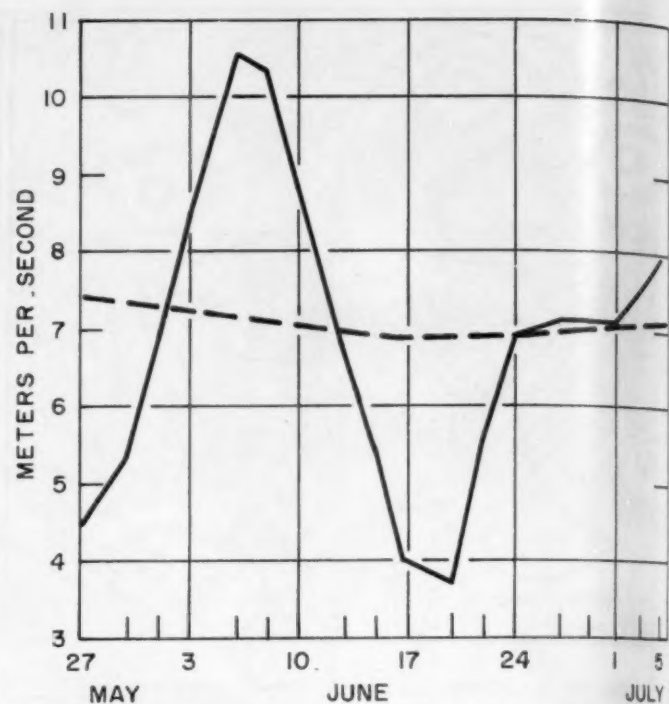


FIGURE 5.—Time variation of the 5-day mean values of the zonal westerlies in meters per second for June 1959, plotted on the last day of the period. The zonal index is computed from 35° to 55° N. for the Western Hemisphere. The minimum on the curve represents the second lowest 5-day mean index of record for June.

air filtered into the Pacific Northwest, and warming occurred from the Southern Plains to Virginia. Patterns for both weeks resembled the monthly mean temperature departure from normal (fig. 9).

Rapid cooling over the eastern third of the Nation, except for a strip along the southeastern corner, followed the onset of blocking in eastern North America the third week. Pressures rose strongly over the Maritime Provinces, cutting off a vigorous Low along the New England coast. Daily record low temperatures were reported this week from the Great Lakes to South Carolina. Frost damage occurred in Indiana, and snow was reported in the mountains of New Hampshire.

During the final week cool air again pushed into the Pacific Northwest and extended eastward to Lake Superior. Blocking relaxed over eastern North America, followed by rapid warming over the Eastern States. The month closed with a heat wave of record intensity along the Atlantic seaboard. New daily high temperature records were established at numerous stations from Columbia, S.C., to Nantucket, Mass., from the 28th through the 30th.

5. PRECIPITATION

In some areas this month's precipitation is more easily related to the mean sea level circulation than to the 700-mb. mean. Where the area was dominated by abnormally warm temperatures, precipitation in excess of normal

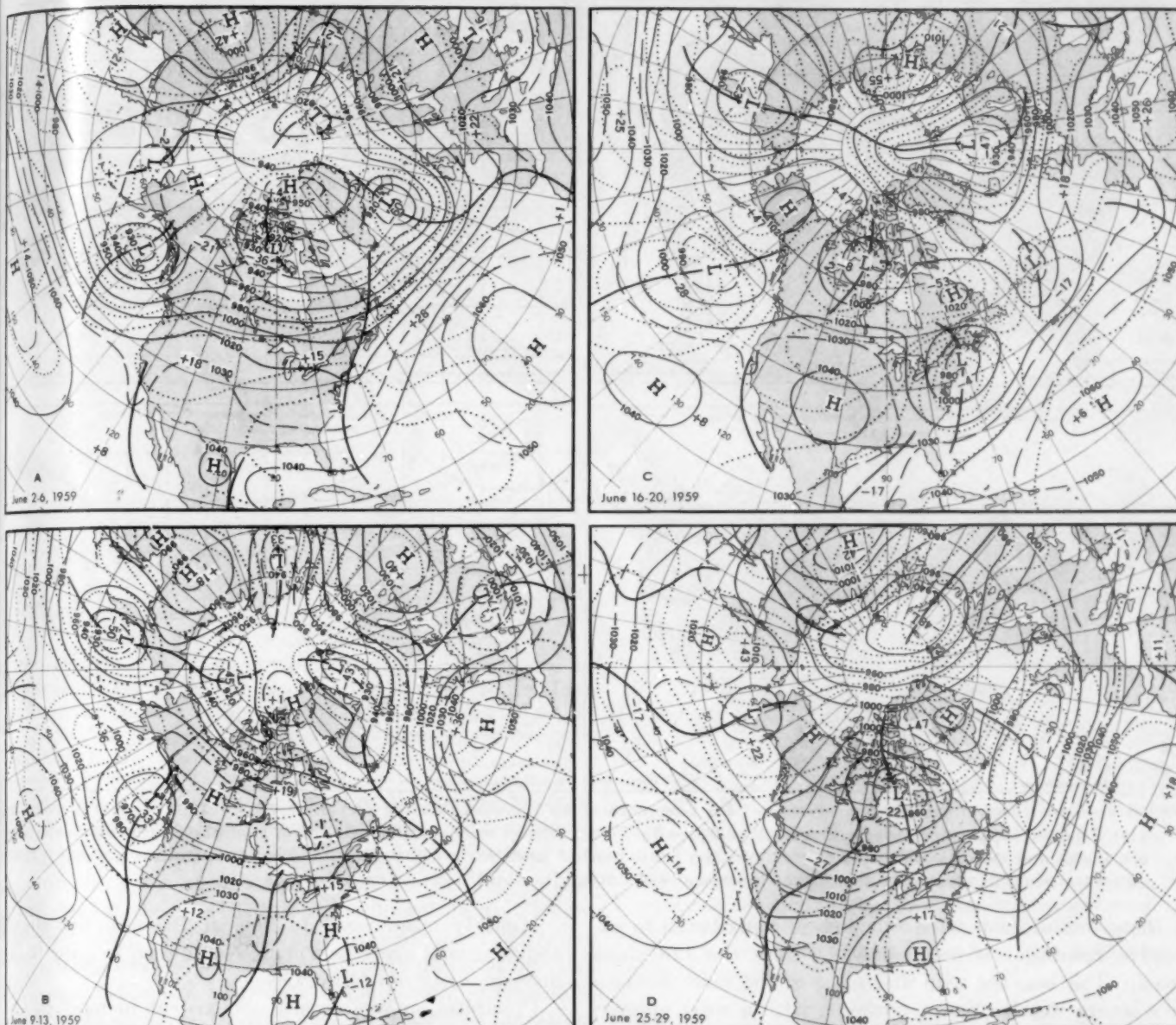


FIGURE 6.—Five-day mean 700-mb. contours (solid) and height departures from normal (dotted) both in tens of feet, for (A) June 2-6, (B) June 9-13, (C) June 16-20, (D) June 25-29, 1959. The zonal index was at its peak early in the month (A), and amplitudes of the mean waves were small. Blocking was most pronounced and the index lowest during the third week (C).

(fig. 10) coincided rather well with cyclonically curved mean sea level flow (fig. 11) from the southeast. The broad belt of southeasterly flow from the Gulf of Mexico provided adequate moisture, especially for orographic rainfall in the mountainous regions of New Mexico, Arizona, and Utah.

Locally severe thunderstorms were reported in the moist air mass over Kansas and Nebraska. A storm near Seldon, Kans., produced hail over a 10-square-mile area, measuring up to 3 feet deep in drifts, and total precipitation was estimated at more than 5 inches. Another severe storm moved over Grand Island, Nebr., where hail described as grapefruit sized was driven by winds up to 8 m.p.h.

A number of frontal waves skirted the western boundary of much-above-normal temperatures from northern Nevada to eastern Montana. Some of these storms were fairly vigorous but not violent, though squall lines in their warm sectors produced locally severe thunderstorms and a few tornadoes. One of the tornadoes occurred near Fargo, N. Dak., on the 9th and another near Green Bay, Wis., on the 10th.

A streak of above normal precipitation from Texas northeastward can be related to a weak mean trough at 700 mb. (fig. 1). Some of the rain in southern Texas was associated with tropical storm Beulah, which threatened the southern Texas coast on the 16th and 17th but moved inland well south of Brownsville.

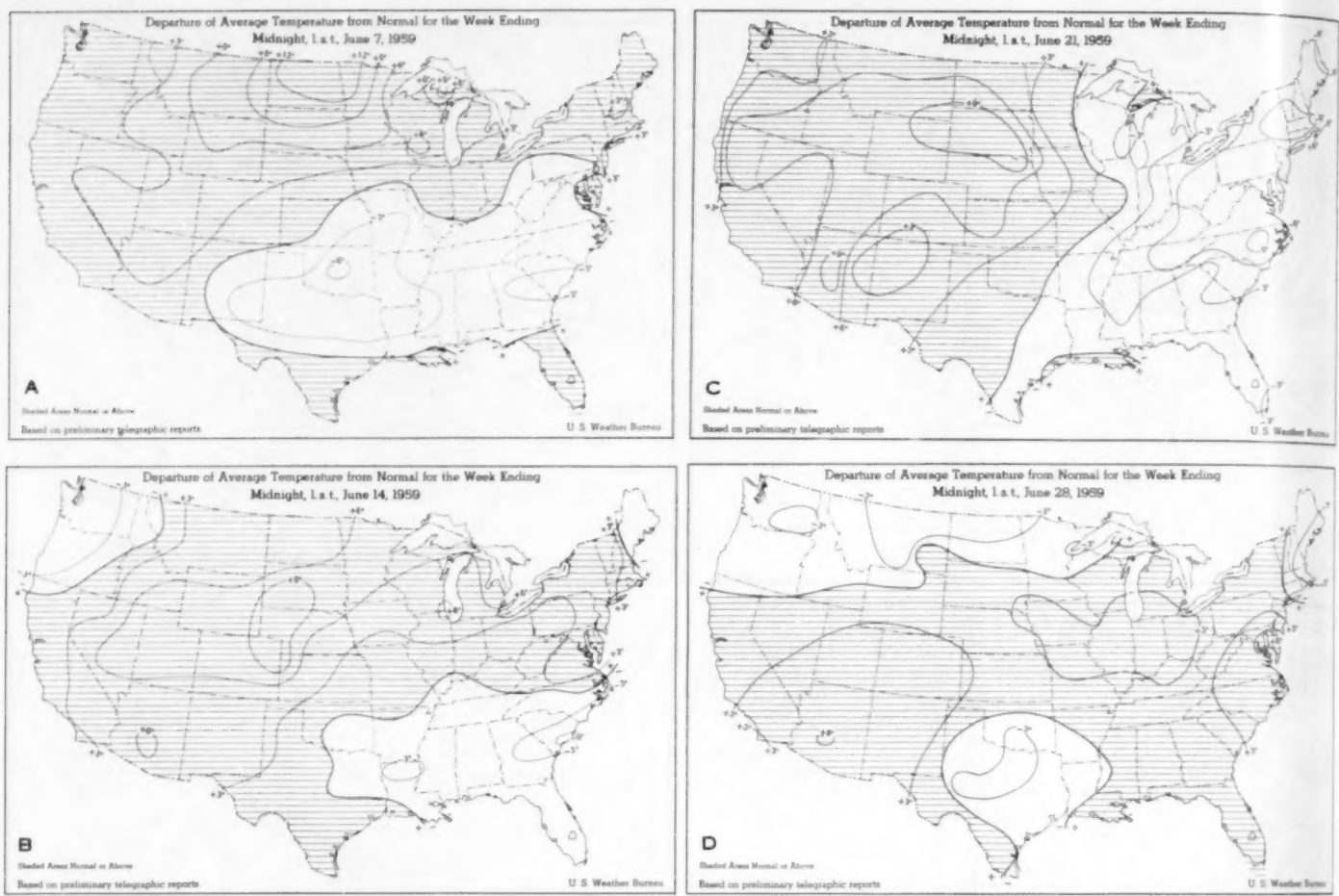


FIGURE 7.—Departures of average temperature ($^{\circ}$ F.) from normal for the weeks ending (A) June 7, (B) June 14, (C) June 21, and (D) June 28, 1959, concurrent with periods of figure 6. Temperatures were continuously warm from the Southwest to the Northern Plains and mostly cooler than normal over the South-Central and Southeastern States. Low temperatures set daily records at several stations from the Great Lakes southeastward during the third week. (From [6].)

Remnants of tropical storm Arlene contributed to excessive rainfall east-northeastward from the Louisiana coast. The heaviest rain and some of the most destructive severe weather came, however, with a weak-appearing tropical depression which crossed Florida on the 18th. This low triggered at least two tornadoes, of which the most severe struck Miami, Fla., on the 17th, injuring about 100 persons, and causing damage estimated at \$1½ million. A second tornado was reported in Palm Beach County but caused no injuries and little damage. Also on the 17th, squalls were reported near Fort Myers, Fla., and 24-hour rainfall at that station totaled 6.64 inches. Totals at Miami Beach and Miami Airport on the 18th were 6.28 and 5.95 inches, respectively. Rainfall was copious as far north as Orlando, where the 2-day total for the 17th and 18th was 4.40 inches.

North of Cape Hatteras much of the excessive rainfall can be attributed to the blocked New England Low, which was deepest during the third week and is reflected in the mean pattern of figure 1 as a negative anomaly center. In New England, Hartford, Conn., reported 22 cloudy days for a new June record and Portland, Maine, 24 cloudy days to equal the alltime record for any month.

Monthly mean westerly flow at 700 mb. was slightly above normal over the Pacific Northwest, helping to produce excessive rainfall in Oregon.

Precipitation was almost nonexistent in most of California and much of Arizona and Nevada, with positive 700-mb. anomalies and weaker than normal mean westerlies across the area. Sacramento, Calif., reported the driest spring in 110 years of record and Oakland the driest June. Drought continued at Tucson, with no measurable rain observed.

Parts of the Midwest were also dry. Springfield, Ill., reported the driest June in 80 years of record, and Detroit, Mich., had its driest June since 1895. Milwaukee, Wis., St. Louis, Mo., and Columbus, Ohio, reported their driest June since the early 1930's. Here the mean circulation was anticyclonic at sea level (fig. 11) and at the 700-mb. level (fig. 1).

6. HAWAII AND ALASKA

From Hawaii and Alaska came reports of warmth and dryness for June. Lihue, Kauai, Hawaii, had this to report [8]: "All of the following temperature values were higher than any previously recorded in the month of

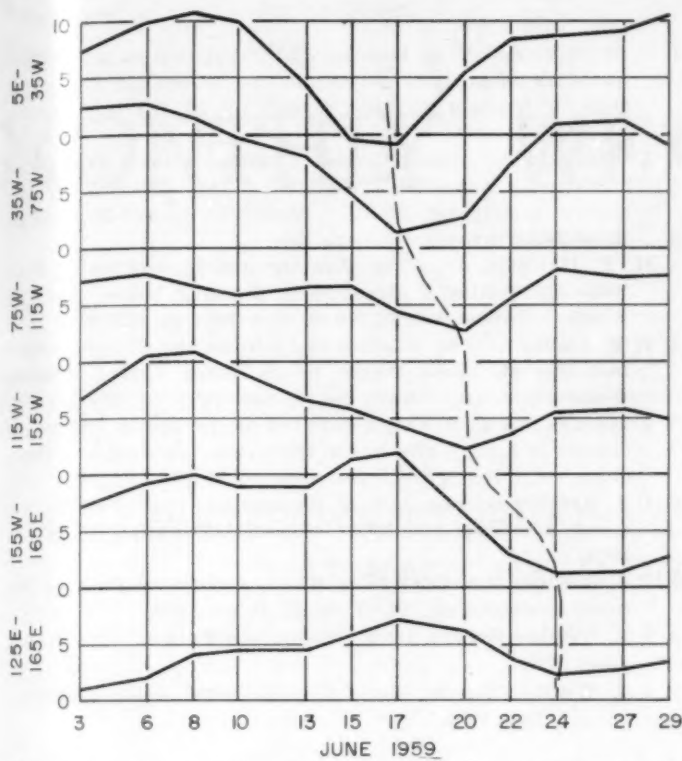


FIGURE 8.—Time variation of the 5-day mean zonal westerlies in regional zones of 40° longitude, in meters per second, for June 1959. Indices were computed for 35° to 55° N. and plotted on the last day of the period. Note the westward progression of minima in the curves during the second half-month.

June: Average Maximum, Average Minimum, Average Monthly, and the Highest for the month. Not only was the previous highest temperature exceeded on 1 day, but the previous record was equaled on 4 other days. Not once during the month did the temperature fall below normal. Dry weather continues over all parts of the island, the dryness being only slightly relieved by the showers on the last two days of the month." Honolulu Airport had only a trace of rain in June, the lowest on record there, and Hilo, Hawaii, reported a deficit from normal of 3.63 inches. The anomalies were associated with somewhat weaker than normal trade wind flow at sea level.

Anchorage, Alaska, reported [9] "Measurable precipitation fell on only 3 days, and totaled only 0.26 inch, less than one-third the normal amount. Thunderstorms are relatively rare in Anchorage, but one occurred on June 25. The mean temperature for the month was 56.6° , 2.9° higher than normal." At Fairbanks the temperature average 2.2° F. above normal; at Juneau, 1.6° F. above normal. Both stations reported thunderstorms and less than normal precipitation for the month.

Warmer than normal temperatures at these Alaskan stations were related in the usual sense to positive 700-mb. height anomalies (fig. 1). Below normal precipitation might be expected with the 700-mb. anomalous flow from the northeast rather than from the usual moisture source in the Gulf of Alaska.

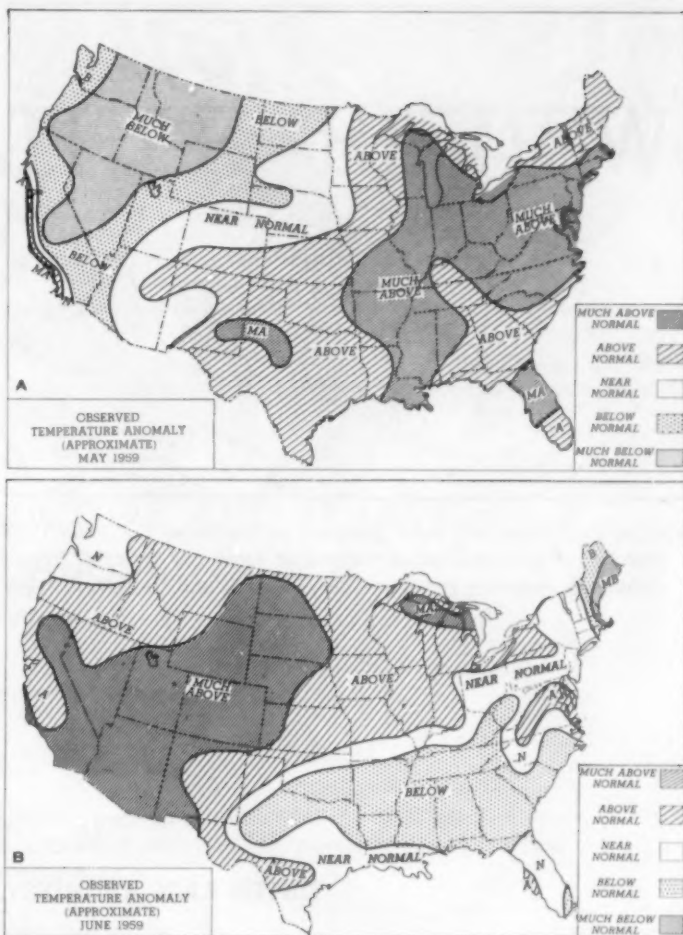


FIGURE 9.—Observed temperature anomaly for (A) May 1959 and (B) June 1959. Normal is established from 30-year averages for the period 1921 through 1950 with normal, below, and above occurring one-fourth of the time. Much below and much above each occur one-eighth of the time. Temperature anomalies in June changed more than one class from May at 60 percent of selected stations.

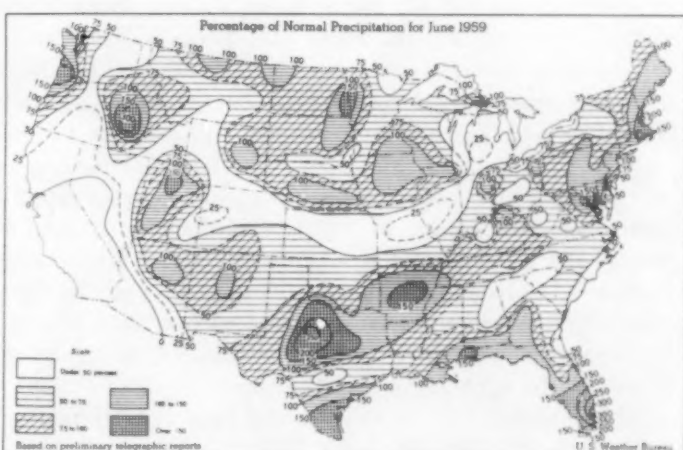


FIGURE 10.—Percentage of normal precipitation for June 1959 (from [7].) Much of the excessive precipitation in the South was related to tropical cyclones.

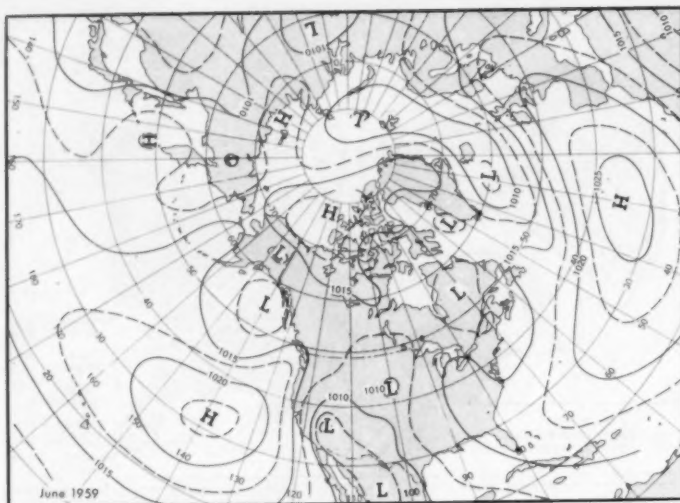


FIGURE 11.—Mean sea level pressure in millibars for June 1959. The broad belt of southeasterly flow from the Gulf of Mexico furnished moisture for numerous showers and thundershowers.

REFERENCES

1. C. M. Woffinden, "The Weather and Circulation of May 1959—Including an Analysis of Precipitation in Relation to Vertical Motion," *Monthly Weather Review*, vol. 87, No. 5, May 1959, pp. 196-205.
2. J. Namias, "The Annual Course of Month-to-Month Persistence in Climatic Anomalies," *Bulletin of the American Meteorological Society*, vol. 33, No. 7, Sept. 1952, pp. 279-285, and an unpublished extension through 1954.
3. H. F. Hawkins, Jr., "The Weather and Circulation of June 1955—Illustrating a Circumpolar Blocking Wave," *Monthly Weather Review*, vol. 83, No. 6, June 1955, pp. 125-131.
4. J. F. Andrews, "The Weather and Circulation of April 1959—Including the Role Played by an Index Cycle," *Monthly Weather Review*, vol. 87, No. 4, Apr. 1959, pp. 153-161.
5. J. Namias and P. F. Clapp, "Studies of the Motion and Development of Long Waves in the Westerlies," *Journal of Meteorology*, vol. 1, Nos. 3 and 4, Dec. 1944, pp. 57-77.
6. U.S. Weather Bureau, *Weekly Weather and Crop Bulletin, National Summary*, vol. XLVI, Nos. 23-26, June 8, 15, 22, 29, 1959.
7. U.S. Weather Bureau, *Weekly Weather and Crop Bulletin, National Summary*, vol. XLVI, No. 27, July 6, 1959.
8. U.S. Weather Bureau, *Local Climatological Data*, Lihue, Kauai, June 1959.
9. U.S. Weather Bureau, *Local Climatological Data*, Anchorage, Alaska, June 1959.

Weather Note

TINTED RAIN AT DUNSTABLE, MASS., JUNE 6, 1959

Robert E. Lautzenheiser

Weather Bureau State Climatologist, Boston, Mass.

Greenish-yellow tinted rain was observed in Dunstable, Mass., at 4 p.m. EST, June 6, 1959. At the height of a thundershower, visibility was reduced at times to 20 feet by heavy rain which appeared to have a greenish tint, according to Edward Hill, Cooperative Weather Observer at Dunstable.

During the morning and afternoon the air over Dun-

stable contained a large amount of a greenish-yellow pollen. Prior to the rain, pollen was deposited on the ground, roofs, and other surfaces. The deposit on the inside of the thermometer shelter was nearly one-sixteenth inch thick. The contents of the rain gage were light green in color, due to a considerable amount of pollen.